AD NUMBER

AD846204

LIMITATION CHANGES

TO:

Approved for public release; distribution is unlimited.

FROM:

Distribution authorized to U.S. Gov't. agencies and their contractors; Critical Technology; NOV 1968. Other requests shall be referred to Rome Air Development Center, Griffiss AFB, NY 13440. This document contains export-controlled technical data.

AUTHORITY

RADC ltr, 17 Sep 1971

RADC-TR-68-349
Final Report

ABSOLUTE GAIN MEASUREMENTS FOR HORN ANTENNAS

Ronald R. Bowman
National Bureau of Standards

TECHNICAL REPORT NO. RADC-TR-68-349
November 1968

Rome Air Development Center
Air Force Systems Command
Griffiss Air Force Base, New York

When US Government drawings, specifications, or other data are used for any purpose other than a definitely related government procurement operation, the government thereby incurs no responsibility nor any obligation whatsoever; and the fact that the government may have formulated, furnished, or in any way supplied the said drawings, specifications, or other data is not to be regarded, by implication or otherwise, as in any manner licensing the holder or any other person or corporation, or conveying any rights or permission to manufacture, use, or sell any patented invention that may in any way be related thereto.

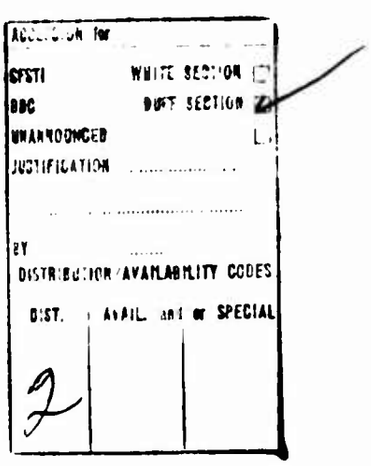

Do not return this copy. Retain or destroy.

ABSOLUTE GAIN MEASUREMENTS FOR HORN ANTENNAS

Ronald R. Bowman

National Bureau of Standards

AFLC, GAFB, N.Y., 27 Dec 65-140

FOREWORD

This final report was prepared by National Bureau of Standards, Institute for Basic Standards, Radio Standards Engineering Division, Boulder, Colorado under Contract No. F30602-67-C-0163, Project 4540, Task 454001. Period of time covered was January 1967 to July 1968.

RADC Project Engineer was James W. Hayes, 1st Lt, USAF (EMCVM-1).

The report summarizes the development of measurement techniques and a detailed technical analysis to provide absolute gain measurements for horn antennas used as gain standards. The measurement techniques described in this report are also suitable for routine gain measurements.

The author is indebted to Dr. R. C. Baird and D. R. Belsher for many helpful discussions and suggestions. He also wishes to thank D. R. Belsher for his assistance with the experimental work and the illustrations.

The distribution of this document is limited under the U.S. Mutual Security Acts of 1949.

This technical report has been reviewed and is approved.

Approved: James W. Hayes
JAMES W. HAYES
1st Lt, USAF
Project Engineer

Approved: Richard M. Cosel
RICHARD M. COSEL
Colonel, USAF
Chief, Communications Division

FOR THE COMMANDER: Irving J. Gabelman
IRVING J. GABELMAN
Chief, Advanced Studies Group

ABSTRACT

A detailed discussion is presented of absolute gain measurements by the insertion-loss method (also known as the "two-antenna" or "three-antenna" method). The discussion emphasizes error analysis, electrical mismatch, near-zone corrections, swept-frequency gain measurements, and techniques for experimentally reducing the effects of multipath interference. Some simple terms, concepts, and formulas are presented that are useful for the design and evaluation of antenna or field strength measurements when multipath interference is involved. It is concluded that swept-frequency gain measurements with uncertainty limits of less than ± 0.1 dB can be made on small indoor ranges for most horn antennas. Examples of horn-gain measurements are included.

TABLE OF CONTENTS

EVALUATION

The research effort described in this technical report has resulted in the development of very accurate microwave horn antenna gain calibration techniques and standards. These will become the basis of a primary calibration service at the National Bureau of Standards and a secondary one within the Air Force calibration laboratory system. In addition, the techniques will be incorporated into a method for the calibration of microwave field intensity meters under another effort presently in progress at NBS. Upon completion of the program, calibration services for microwave antenna gain and field intensity will be available to support RFI and system performance measurement programs.

James W. Hayes 1/LT

JAMES W. HAYES, 1st Lt, USAF
Effort Engineer

ABSOLUTE GAIN MEASUREMENTS FOR HORN ANTENNAS

by

Ronald R. Bowman

1. Gain Measurements by the Insertion-Loss Method.

1.0 Introduction.

The measurement method that will be discussed here is usually referred to as the "three-antenna" method or, when measuring the gain of two identical antennas, the "two-antenna" method. For reasons that will be obvious, the term "insertion-loss" is felt to be more descriptive of this method. Familiarity with this method is assumed, but it will be reviewed to emphasize the requirements for accurate gain measurements. The discussion will be with respect to gain measurements of horn antennas with uncertainty limits† in the range ±0.1 to ±1.0 dB.

† That is, the limits of the "likely" departure from true values[18]. As used here, "likely" means that the "probability" (assumed, calculated, guessed, estimated, or otherwise determined) is about 99 percent or more that the true value of the measurand is within the stated limits.

1.1 The Insertion-Loss Method.

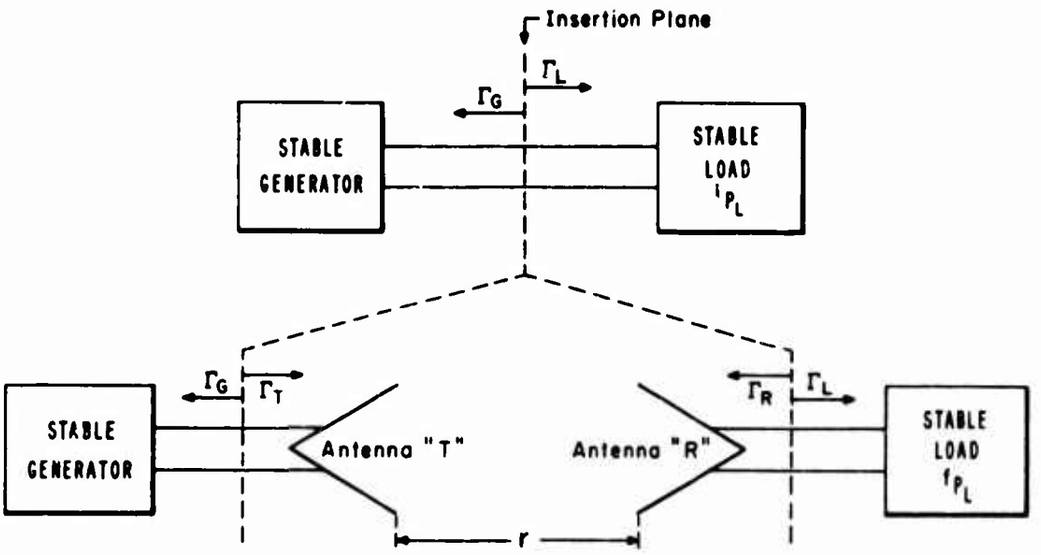

Figure 1. Schematic Representation of an Insertion-Loss Measurement.

The basic procedure for this method is essentially the same as that for measuring the attenuation of a waveguide† attenuator. Referring to Figure 1, the generator and load are connected and a reference power level is recorded. Then the antenna transmission path is "inserted" by coupling the generator and load to the antennas (previously oriented) and the change in power level is recorded. Thus, this method of measuring antenna gain is a particular case of an insertion-loss measurement.[1,2,4]

Ignoring mismatch losses for the moment, the initial load power is equal to the power delivered to the transmitting antenna and the final load power is the power received by the receiving antenna.

†Following the recommended IEEE definition, "waveguide" refers to any RF transmission line. If it is necessary to make a distinction, such terms as "hollow waveguide" or "coaxial waveguide" will be used.

In order to eliminate or evaluate the effects of electrical mismatch† it is necessary to have a "working" formula that is valid for arbitrary matching of the generator, load, and antennas. Obviously, the "initial" matching between the generator and load will affect the measurement, as will the "final" matching between the generator and transmitting antenna and between the load and receiving antenna. If G_T is the gain function of the transmitting antenna and G_R is the gain function of the receiving antenna, it can be shown[3] that, under the conditions listed on page 4,

$$G_T G_R = \left[\frac{|1-\Gamma_g\Gamma_T|^2 \; |1-\Gamma_R\Gamma_L|^2}{(1-|\Gamma_T|^2)(1-|\Gamma_R|^2)\,|1-\Gamma_c\Gamma_L|^2}\right]\left(\frac{4\pi r}{\lambda}\right)^2\left(\frac{{}^fP_L}{{}^iP_L}\right) \qquad (1)$$

where λ is the wavelength, r is the aperture-to-aperture separation distance, ${}^iP_L$ is the power delivered to the load when the generator and load are directly coupled, ${}^fP_L$ is the power delivered to the load when the transmission path is "inserted" between the generator and load, and ${}^fP_L/{}^iP_L$ is the insertion-loss ratio.†† The reflection coefficients Γ_g, Γ_L, Γ_T, and Γ_R refer, respectively, to the generator, load, transmitting antenna, and receiving antenna. (Hereafter, unless stated otherwise, it should be understood that "G" and "gain" refer to the maximum value of a gain function).

If the gain of one of the antennas is known or if the antennas are identical, the unknown gain can be calculated directly from (1). To determine the gains of two antennas that are not identical, a third antenna must be employed. The gains of all three antennas can be established by repeating the insertion-loss procedure three times to determine the products G_1G_2, G_1G_3, G_2G_3 and solving for the gains algebraically. If the gain of the third antenna is not desired, it may be easier instead to determine the product G_1G_2 by the insertion-loss method and determine the ratio G_1/G_2 by the comparison method using the third antenna merely as an illumination source. For simplicity, the discussion in this report centers around the measurement of two identical antennas.

† Since the gain of antennas is defined with respect to complex-conjugate matching, the term "mismatch" will refer to this type of matching (rather than, for instance, "reflectionless" matching).

†† As used here, the insertion-loss ratio (${}^fP_L/{}^iP_L$) is related to the insertion-loss as follows: Insertion-loss = $-10\,\mathrm{Log}\,({}^fP_L/{}^iP_L)$.

The essential conditions[4,6] involved in (1) can be summarized by grouping them as follows:

1) Antenna range -- "infinite" antenna separation; free-space conditions.

2) Equipment -- ideal waveguide leads and connectors; stable generator and load; single sinusoidal frequency; single waveguide mode.

3) Antennas -- reciprocal; polarization parameters matched.[5]

4) Transmitting medium -- linear, lossless, reciprocal, and isotropic.

It should be emphasized that the conditions listed above are necessary for the validity of (1), that is they refer to the assumptions made in deriving (1). Insofar as these conditions constitute a complete list, all of the other sources of uncertainty in the gain measurement are "instrument" uncertainties that result from measuring the quantities in (1).

The stability referred to under conditions 2) requires that the electrical characteristics of the generator and load must be stable despite the physical movements that take place during the insertion-loss measurement and despite the changes in the powers absorbed by the generator† and load. Also the "free-space" condition requires that there be no other source of radiation (radio frequency interference) in addition to requiring that there be no scattering objects (multipath interference). Furthermore, "ideal" waveguide leads and connectors are not only uniform and lossless but also have zero leakage.

Some of the conditions listed above are usually automatically satisfied to a high degree. For frequencies below about 40 GHz, at least, air can be considered to be an essentially perfect approximation to conditions 4) over the distances necessary for gain measurements of small or moderate sized antennas (say less than 30 dB gain). Also, of course,

† For instance, see pages 27 and 28.

an assumption of perfect reciprocity for horn antennas does not involve significant[†] error, and the usual assumption of a single waveguide mode is considered "safe" if the waveguides are operated within their recommended frequency range.

1.2 Discussion of Errors.

Because there are many sources of error in absolute gain measurements, it is almost necessary to rewrite (1) so that the sources of error are more apparent. Suppose that G_T and G_R are restricted to represent only the maximum values of the gain functions for the transmitting and receiving antennas, and let D be a function that expresses the dependence on the direction angles of the antenna axes (D is the product of the normalized directivities). Furthermore, let R be a function that expresses the dependence on the polarization matching[5,6] of the antennas (R is a function of the polarization parameters of each antenna and the rotation about each antenna axis), and let M equal the mismatch term of (1). Then from (1),

$$(G_T G_R)(DR) = M\left(\frac{4\pi r}{\lambda}\right)^2 \left(\frac{{}^f P_L}{{}^i P_L}\right) \tag{2}$$

Now let N be a correction factor for insufficient antenna separation, and let ${}^f P_{L0}$ be the "signal" or "free-space" load power (i.e. the power that would be delivered to the load under perfect free-space conditions). Then, to a good approximation, [††]

$$G_T G_R = \left(\frac{MN}{DR}\right)\left(\frac{4\pi r}{\lambda}\right)^2 \left(\frac{{}^f P_{L0}}{{}^i P_L}\right) \tag{3}$$

[†] The word "significant" must be interpreted with respect to the total uncertainty limits for a given gain measurement. Roughly speaking, an individual source of error should be considered significant if its uncertainty limits are larger than a few percent of the (anticipated) total uncertainty limits.

[††] Strictly speaking, N, D, and R may not be separable functions.

To some extent (3) is meant to be a "memory device" to aid in analyzing the many sources of error in absolute gain measurements; however, it should not be thought that (3) is merely a memory device since explicit formulations for M, N, D, R can be (and have been) derived and expressions for ${}^{f}P_{L\theta}$ can, in principle at least, also be derived. (An expression for M is included in this paper, and expressions for R are fairly well-known[5,6]). The usefulness of (3) lies in the fact that its validity is dependent on only three conditions that are likely to cause significant uncertainties for horn gain measurements with total uncertainty limits $> \pm 0.1$ dB. These conditions are: (a) ideal waveguide leads and connectors, (b) stable generator and load, and (c) single sinusoidal frequency. Thus, if the limitations stated at the end of Section 1.1 are not exceeded, an error analysis that assigns uncertainty limits to all of the variables in (3) plus uncertainty limits for violations of (a), (b), and (c) can be considered to be essentially complete in that it does not leave out any commonly recognized sources of uncertainty larger than 0.01 dB.

With three exceptions, it will be assumed that the necessary procedures for determining the quantities on the right in (3) are either obvious or are well-known. The procedures for determining M, N, and ${}^{f}P_{L\theta}$ † are discussed in Sections 2, 3, and 4. Further discussion of errors can be found in these sections and also in Section A1, which contains examples of gain measurements.

---

† Since only the ratio of the final and initial load powers is needed, absolute power measurements are not required. The signals actually recorded during a gain measurement need only to be related to the load powers in such a way that the insertion-loss ratio can be determined. For instance, in Section A1 the recorded signals are proportional to the decibel value of the load power. However, there is no essential difference in procedure, by the method to be discussed, in determining the "free-space" value of a signal produced by the load power and determining the "free-space" value of the actual load power; and for convenience of discussion it will be assumed that ${}^{f}P_{L\theta}$ is being determined.

2. Mismatch

2.1 Using Tuners to Reduce Mismatch.

For antennas that are to be operated at one frequency only, it is common to connect tuners as permanent parts of the antennas so that the reflection coefficients of the antennas can be reduced or made negligibly small. If tuners are also incorporated with the generator and load so that Γ_G and Γ_L can be "tuned out", the mismatch factor M can be made very nearly equal to unity.

An alternative practice is to incorporate tuners with the generator and load only. These tuners are then adjusted for maximum load power when measuring ${}^{i}P_L$ and ${}^{f}P_L$. This procedure involves an error, probably small, because the dissipative losses of the tuners will be different for the initial and final load power measurements (i.e. the generator and load will not be stable).

2.2 Calculating Mismatch Corrections.

If gain measurements are to be made at many frequencies within a band or if swept-frequency gain measurements are to be made, it will be difficult or impossible to use tuners to provide matched conditions. It will then be necessary, for accurate measurements, to at least partially evaluate

$$M = \frac{|1-\Gamma_G\Gamma_T|^2 \; |1-\Gamma_R\Gamma_L|^2}{(1-|\Gamma_T|^2)\,(1-|\Gamma_R|^2)\,|1-\Gamma_G\Gamma_L|^2} \qquad (4)$$

from known reflection coefficients. Since instruments are commercially available that can measure reflection coefficients (magnitude and phase) on a swept-frequency basis and since (4) can be easily programmed for automatic calculation, a complete evaluation of M can be made fairly easily even for swept-frequency gain measurements. However, it will often be sufficient to know only the magnitudes of the reflection

coefficients in the mismatch factor.

If the magnitudes of the reflection coefficients are known then M can obviously be partially determined from

$$M = \left[\frac{1}{(1-|\Gamma_T|^2)(1-|\Gamma_R|^2)}\right]\left[\frac{(1\pm|\Gamma_G||\Gamma_T|)^2\,(1\pm|\Gamma_R||\Gamma_L|)^2}{(1\mp|\Gamma_G||\Gamma_L|)^2}\right] \qquad (5)$$

The right hand side of (5) has been written as two factors to emphasize that the first factor is essentially a partial correction factor for mismatch while the second factor merely gives the upper and lower limits for the corresponding terms in (4). If the $|\Gamma|$'s in (5) are all small, then M can be calculated approximately from

$$M \approx \left[1 + |\Gamma_T|^2 + |\Gamma_R|^2\right] \pm 2\left[|\Gamma_G||\Gamma_T| + |\Gamma_R||\Gamma_L| + |\Gamma_G||\Gamma_L|\right]. \qquad (6)$$

If all of the $|\Gamma|$'s are less than 0.2 (VSWR < 1.5) then the first term of (6) is about 0.5 percent (about 0.02 dB) smaller than the first factor of (5) and the maximum and minimum values of M calculated from (6) are within 5 percent (0.2 dB) of the same values calculated from (5). If all of the $|\Gamma|$'s are less than 0.1 then the first term of (6) is about 0.03 percent (about 0.0015 dB) smaller than the first factor of (5) and the maximum and minimum values of M calculated from (6) are within 0.4 percent (0.02 dB) of the same values calculated from (5).

2.3 Estimating the Limits of Uncertainty for Mismatch.

For crude gain measurements, the mismatch factor M can be used merely to estimate limits of uncertainty for mismatch. Within the frequency band of interest, the maximum value of the magnitude of each reflection coefficient is determined by estimate or from specified performance data for the various waveguide components, and estimates for the maximum possible limits of uncertainty are calculated from these values. Because good quality waveguide components have reflection

coefficient magnitudes no larger than about 0.2, approximation (6) can be used for this calculation. It should be noted that it is also necessary to assign minimum values to $|\Gamma_T|$ and $|\Gamma_R|$ when calculating the lower limit for M. Therefore, for any frequency within the band,

$$M_u = 1 + |\Gamma_T|_u^2 + |\Gamma_R|_u^2 + 2|\Gamma_G|_u|\Gamma_T|_u + 2|\Gamma_R|_u|\Gamma_L|_u + 2|\Gamma_G|_u|\Gamma_L|_u \quad (7)$$

$$M_\ell = 1 + |\Gamma_T|_\ell^2 + |\Gamma_R|_\ell^2 - 2|\Gamma_G|_u|\Gamma_T|_u - 2|\Gamma_R|_u|\Gamma_L|_u - 2|\Gamma_G|_u|\Gamma_L|_u \quad (8)$$

where the subscripts u and ℓ designate, respectively, the upper and lower limits of each quantity. Typically, $|\Gamma_R|_\ell$ and $|\Gamma_T|_\ell$ will be small and it is convenient to assume that they are zero.

2.4 A Commonly Used Method for Achieving a Low-Reflection Generator.

For accurate measurements it is nearly always necessary to use a "leveled" generator to provide adequate power stability. The recommended and commonly used practice is to use a directional coupler for the output component of the generator so that the leveling signal can be derived from the nearest possible point to the output port (see Fig. 5 in Section A1). This practice usually provides minimum power variation with respect to frequency and also can provide a low-reflection generator.[7,8] The maximum possible reflection coefficient magnitude of the equivalent generator is given by

$$|\Gamma_{GE}|_{max} = |S_{22}| + 10^{-(d/20)} \quad (9)$$

where S_{22} is the reflection coefficient "looking into" the output port of the directional coupler as measured with the other two arms connected to reflectionless loads and d is the directivity of the coupler expressed in dB.

This method for achieving a low-reflection generator is particularly important when making swept-frequency gain measurements because it provides a generator that is automatically tuned to be "reflectionless" during the sweep. However, for very accurate swept-frequency gain measurements it may be necessary to accurately measure the phase as well as the magnitude of Γ_{gg}; and then this method is not practical because, due to the finite directivity of the coupler, Γ_{gg} will be a function of the magnitude and phase of the voltage wave incident on the generator port. It is fairly easy, though, to measure $|\Gamma_{gg}|$.[7,8] (If it is necessary to know both the magnitude and phase of Γ_g for swept frequency measurements, best practice is to use an attenuator or isolator for the output component of the generator to insure that Γ_g will be stable.)

2.5 Reducing the Effects of Mismatch by Experimental Techniques.

It is possible to reduce the effects of internal reflections by the same techniques used to reduce the effects of external "reflections" (see Section 4). For instance, suppose that the load consists of a long piece of essentially perfect waveguide terminated in a detecting element. Insofar as the waveguide is perfect, $|\Gamma_L|$ will be determined solely by the discontinuity at the detecting element. The phase of Γ_L will change rapidly as the frequency is swept, and periodic variations in the load power will result that correspond to the two terms in M that contain Γ_L. These terms can then, in effect, be eliminated by averaging out these variations. (For further discussion of this technique see Reference 15). For gain measurements the value of this technique is somewhat questionable because it will complicate the process of reducing the effects of multipath interference by the swept-frequency technique, which may substantially increase the uncertainty limits for $^fP_{L0}$; and the swept-frequency technique is usually much more valuable for determining $^fP_{L0}$ than it is for "eliminating" terms in the mismatch factor. However, if carefully

employed, this technique can sometimes substantially reduce the effort of evaluating the effects of mismatch.

Obviously, "line-stretchers" can also be used to cause phase changes so that the effects of troublesome internal reflections can be averaged out, and this technique is directly analagous to the "antenna movement" technique described in Section 4 for averaging out the effects of multipath interference. Provided that the line-stretcher itself is essentially "reflectionless", this technique may sometimes be useful.

3. Near-Zone Corrections

3.1 Definition of the Near-Zone.

Consider an antenna radiating into free-space. In any given direction, the power radiated per unit solid angle varies, reaching an asymptotic value with increasing distance. Now, if a receiving antenna is introduced at some location far enough from the transmitting antenna that the power densities per unit solid angle radiated to that location do not differ significantly from the corresponding asymptotic values, the receiving antenna is, by definition, located in the far-field region of the transmitting antenna. It is emphasized, however, that even if the receiving antenna is in the far-field of the transmitting antenna, the (unperturbed) field at the location of the receiving antenna can still differ significantly from a uniform plane-wave field. Then, the power transmission cannot be simply expressed in terms of the far-field gain functions of the antennas; and, as defined here, the receiving antenna is in the near-zone region. (Note that the near-zone, in contrast to the near-field, is determined by the characteristics of both antennas.) The near-zone includes the near-field and often is much more extensive than the near-field.

It should be noted that the much misused formula $r = 2a^2/\lambda$[†] for determining "adequate" range distances is applicable only for estimating the extent of the near-field in the direction of maximum radiation of antennas

[†] For circular apertures, "a" is the diameter; for rectangular apertures, "a" is the larger dimension.

that have zero "phase error".[3,9] (Even then, this estimation formula is not useful for high accuracy antenna measurements). Horn antennas usually have large "phase error", and an adequate separation distance for far-zone power transfer between two such identical horns is typically larger than $r = 10a^2/\lambda$.[3,9]

3.2 Determining Near-Zone Corrections.

Several calculations have appeared[9,10,11] for corrections that can be used for pyramidal horn gain measurements made in the near-zone. Unless an outdoor range with tall towers is available, it is difficult to make accurate horn gain measurements without using these corrections because multipath interference problems are relatively severe when the antennas are located in the far-zone region. For an error of less than 0.1 dB, a typical separation distance for a horn gain measurement would have to be about $10a^2/\lambda$. By making use of near-zone corrections, accurate gain measurements can be made with separation distances as small as a^2/λ.

The near-zone correction calculated by Braun[9] is limited to gain measurements using identical pyramidal horns, and it involves some approximations that were not made in the later calculations by Chu and Semplak[10] and by Tseytlin and Kinber[11]. Braun's calculation differs substantially from the later calculations and should no longer be used.

Chu and Semplak's calculation is also limited to the case of identical pyramidal horns. The tabular correction data from Chu and Semplak's calculation is graphed in Section A4. This section also contains some graphs showing correction factors determined by Chu and Semplak's data for some of the commonly used "NRL" design[12] horns.

The results of Tseytlin and Kinber's calculation, which are not reproduced here, are in a form that is relatively difficult to use; but this calculation is important because it is applicable to the power transmission between two different pyramidal horns. The use of Tseytlin

and Kinber's results is straightforward, but a considerable amount of algebraic computation is involved.

For non-pyramidal horns, large separation distances must be used for gain measurements until near-zone correction data has been calculated for such horns. Near-zone correction data can be calculated for power transmission between any two horns provided that the aperture field for each horn is known.[10,11,13] It is likely that calculations will soon be made for conical horns and for horns with flared sides.

3.3 An Estimate of the Accuracy of the Near-Zone Corrections.

It has not yet been possible to calculate limits of error for the near-zone corrections, and in a recent review of the literature[3] it was concluded that experimental confirmation of these corrections was limited to uncertainty limits of about ±10% of the decibel value of the correction for separation distances $r > 2a^2/\lambda$. More recently, an accuracy of 10% or better at $r = a^2/\lambda$ was demonstrated for Chu and Semplak's near-zone corrections.† There are some reasons for believing that these corrections are considerably more accurate than ±10%, and an estimate of ±5% uncertainty limits for $r > 2a^2/\lambda$ is considered, by this author, to be reasonable though not conservative.[14]

It should be mentioned that Tseytlin and Kinber's near-zone corrections for identical horns appear to be appreciably different from Chu and Semplak's for $r < 2a^2/\lambda$.[3] Until Tseytlin and Kinber's calculations have received more complete verification, their use is not recommended for $r < 2a^2/\lambda$.

---

† Unpublished measurements made by the author at the National Bureau of Standards, Boulder, Colorado. These measurements were made with antennas of the "NRL" design (see reference 12) for the frequency range 3.950 to 5.880 GHz.

4. Multipath Interference

4.0 Introduction.

The usual approach to multipath interference (MPI) problems is to try to reduce the MPI to a negligible level by using tall towers, diffraction fences, radiation absorbing materials, and baffles. Another approach is to discriminate against the MPI by using short pulse techniques or doppler frequency shifts. These approaches involve unnecessary complications and expenses that can be avoided, for horn gain measurements at least, by using a third approach, which is to also concentrate on making the effects of MPI easily measurable rather than merely concentrating on discriminating against MPI or reducing it to a negligible level.

Except when measuring very large antennas, it is usually possible to design a range so that the indirect radiation arriving at the receive travels by a considerably longer path than the direct radiation. Then it should be possible, by moving the receiving antenna† or by sweeping the generator frequency, to cause reversals in the relative phases between the component voltage at the load due to the direct radiation field and the component voltages due to the indirect radiation fields.[3,15] If the voltages corresponding to the indirect radiation fields are not too large, the load voltage (or load power) that would result from free-space conditions can be determined by simply averaging out the resulting perturbations in the load voltage (or load power). By using this approach, especially in conjunction with the use of near-zone corrections, it is possible to make accurate gain measurements on a range of minimum size and cost and with minimum expenditure of time and effort. For most horns in common use, $a^2/\lambda < 2$ meters. For such horns, accurate gain measurements can be made in an inside space of about 3 meters by 3 meters by 3 meters with minimal use of radiation-absorbing material.

† For simplicity of discussion, only receiver movements are mentioned here, but it may sometimes be necessary or desirable to employ transmitter movements or movements of surrounding objects.

Note: Unless the reader is familiar with the techniques of using antenna movements or frequency sweeps to evaluate multipath interference, he should read Section A1 before reading the remainder of Section 4.

4.1 Some General Considerations.

Ideally, the magnitude of each interference voltage should remain constant and the phase of each interference voltage should change smoothly and uniformly during the frequency sweep or antenna movement. Then, if the interference voltages are all small, the frequency sweep or antenna movement will result in perturbations in the load power that are essentially a sum of sinusoidal variations around the free-space load power.[†] From the discussion in Section A2 it follows that if the total perturbation in P_L[††] is less than 1.0 dB, peak-to-peak, then P_{L0} can, theoretically, be obtained with less than 0.016 dB error by simply averaging out the perturbations in P_L. In practice, of course, the variations in P_L may be so irregular that the averaged value of P_L may be quite different than P_{L0}. However, with careful design of the gain measurement, the averaged value of P_L will closely approximate P_{L0}.

Because it is so important that the perturbations in P_L be regular, it should be emphasized that many of the techniques commonly used to minimize multipath interference will tend to produce irregular perturbations in P_L. Special precaution is advisable when considering the use of baffles or screening fences since these will produce a lower level of interference only at the expense of increased complexity of interference,

---

[†] This follows from an expansion of Equation (13), See Reference 3.

[††] In Section 4 the superscript "f" will be deleted from ^fP_L and $^fP_{L0}$.

and it is by no means certain that the measurement of P_{L0} will be made simpler or more precise by using these devices. Another common technique that is of questionable value is the practice of using the minima of the antenna patterns to reduce the MPI level at the load. If sources of interference are located along the directions of the minima, it is obvious that the corresponding interference voltages may change so radically as the receiver is moved or as the frequency is swept that it may be difficult to accurately analyze the resulting load power perturbations.

4.2 Determining the Free-Space Load Power.

It is a practical necessity that a continuous reading of P_L be made during the frequency sweep or antenna movement, and P_{L0} can then be easily determined by graphical averaging[†] (see Fig. 6 in Section A1 for instance[††]). The accuracy of the averaging process should be evident by inspection of the recording unless the perturbations are too irregular.

The swept-frequency technique is easiest to employ and has the great advantage of providing wide-band, continuous gain measurements. Unfortunately, the perturbations in the load power are usually relatively irregular for frequency sweeps (see Fig. 6) as compared to the perturbations that result from receiver movements (see Fig. 10). This

---

[†] An alternative would be to digitize the load power signal and use an electronic computer to smooth out the perturbations. This approach would presumably provide greater accuracy, but the main advantage would be that the resulting data would be digitized and ready for automatic calculation of the gain values.

[††] The symbols ${}^{1}S$, ${}^{f}S$, and ${}^{f}S_0$ used in Figures 6, 8, and 10 are explained on pages 36 and 38.

difficulty is not serious, except for gain measurements of the highest accuracy, provided that the load power variations due to the internal reflections of the waveguide system are not confused with the variations due to MPI. In general, if the lengths of the waveguide components and the lengths of the horns are much smaller than the path-length differences for the multipath field components, then it will be quite easy to recognize the power variations that are due to MPI. Best practice is to couple the components of the generator and load directly together† (though, of course, a length of waveguide used between the signal source and a leveling coupler is of no consequence). For further details see Section 4.1.5.

The antenna-movement technique is more "straightforward" than the swept-frequency technique and will generally provide a more accurate determination of P_{L_0}. However, the antenna-movement technique requires much more time and effort to completely characterize the gain of a horn over its full band. Furthermore, this technique requires a mechanism that will produce a smooth movement of at least one of the antennas. As discussed in the next section, the best direction of movement will be along the transmission axis (except, perhaps, when making measurements in the far-zone); and this movement is easily provided by a pedestal or tower that slides or rolls along a pair of rails. It is important that the entire pedestal or tower move rather than just the antenna so that perturbations will be produced in P_L for the multiple scattering between the antennas and pedestals. Also, it may be necessary to move both antennas to completely evaluate the MPI. For instance, suppose that a scattering object that does not move with the receiver pedestal is located close behind the receiver and is illuminated by the main lobe of the transmitter pattern. The field "back-scattered" from this object to the transmitter and then "rescattered" to the receiver can easily be intense enough to cause a significant interference voltage at the

† For an alternative approach, see Section 2.5.

load. If the receiver is moved, the component voltages at the load due to the direct field and this re-scattered field will change in phase by the same amount. Therefore, it will be necessary to move the transmitter also. This difficulty can usually be avoided by shielding such objects with high-performance radiation-absorbing materials.

It is evident that the techniques outlined here must be employed carefully to achieve accurate results. To determine the range requirements and to evaluate the measurements, it is essential to be able to estimate, even if only crudely, both the magnitude and period of the perturbations in the load power that will result from the antenna movements or frequency sweep. Some simple terms, concepts, and formulas are presented in Sections 4.3 and 4.4 that are very useful for designing and evaluating antenna or field strength measurements when small but significant MPI is involved.

4.3 Definitions and Concepts.

If each component of a multipath field is considered separately, the resultant voltage at the load of an antenna immersed in the multipath field will be the phasor sum of the load voltages that would occur from each of these component fields alone, as in (10) (where $\tilde{V}_0$ is the voltage component corresponding to the direct radiation field). The relations and definitions that follow are self evident: †

† It should be emphasized that relations (10) through (13) are not introduced here for purposes of calculation since P_{L0} can usually be determined with satisfactory accuracy by graphical means. Relations (10) through (13) are introduced here because they are necessary for providing unambiguous definitions of the multipath interference parameters.

$$\tilde{V}_L = \tilde{V}_{L0} + \tilde{V}_{L1} + \tilde{V}_{L2} + \ldots \tag{10}$$

$$\tilde{V}_L = \tilde{V}_{L0}(1 + \tilde{K}_1 + \tilde{K}_2 + \ldots) \tag{11}$$

$$\tilde{V}_L = \tilde{V}_{L0}(1 + \kappa_1 e^{j\delta_1} + \kappa_2 e^{j\delta_2} + \ldots) \equiv \tilde{V}_{L0}\tilde{F} \tag{12}$$

$$P_L = P_{L0}\,\tilde{F}\tilde{F}^* \tag{13}$$

$$\tilde{K}_n \equiv \frac{\tilde{V}_{Ln}}{\tilde{V}_{L0}} \equiv \left|\frac{\tilde{V}_{Ln}}{\tilde{V}_{L0}}\right| e^{j\delta_n} \equiv \kappa_n e^{j\delta_n}, \quad n = 1, 2 \ldots$$

(In the following definitions, and elsewhere, identifying subscripts are implied when not stated explicitly.)

$\tilde{K}_n$ = interference coefficient (for component "n")

$\kappa = |\tilde{K}|$ = interference voltage level

δ = phase difference (relative to $\tilde{V}_0$)

$k = 20 \log \kappa$ = interference power level

$\rho = \dfrac{1 + \kappa}{1 - \kappa}$ = voltage interference ratio (VIR)

$p = 20 \log \rho$ = power interference ratio (PIR)

P_{L0} = primary power, signal power, or "free-space" power.

The quantities κ, k, ρ, and p can be related in a convenient graph, as shown in Fig. 2. The dotted lines in this figure indicate how an interference power level of -40 dB is related to the other quantitites. (Interference power levels are usually easier to estimate than interference voltage levels because antenna patterns and reflectivities of materials are generally stated in decibels.)

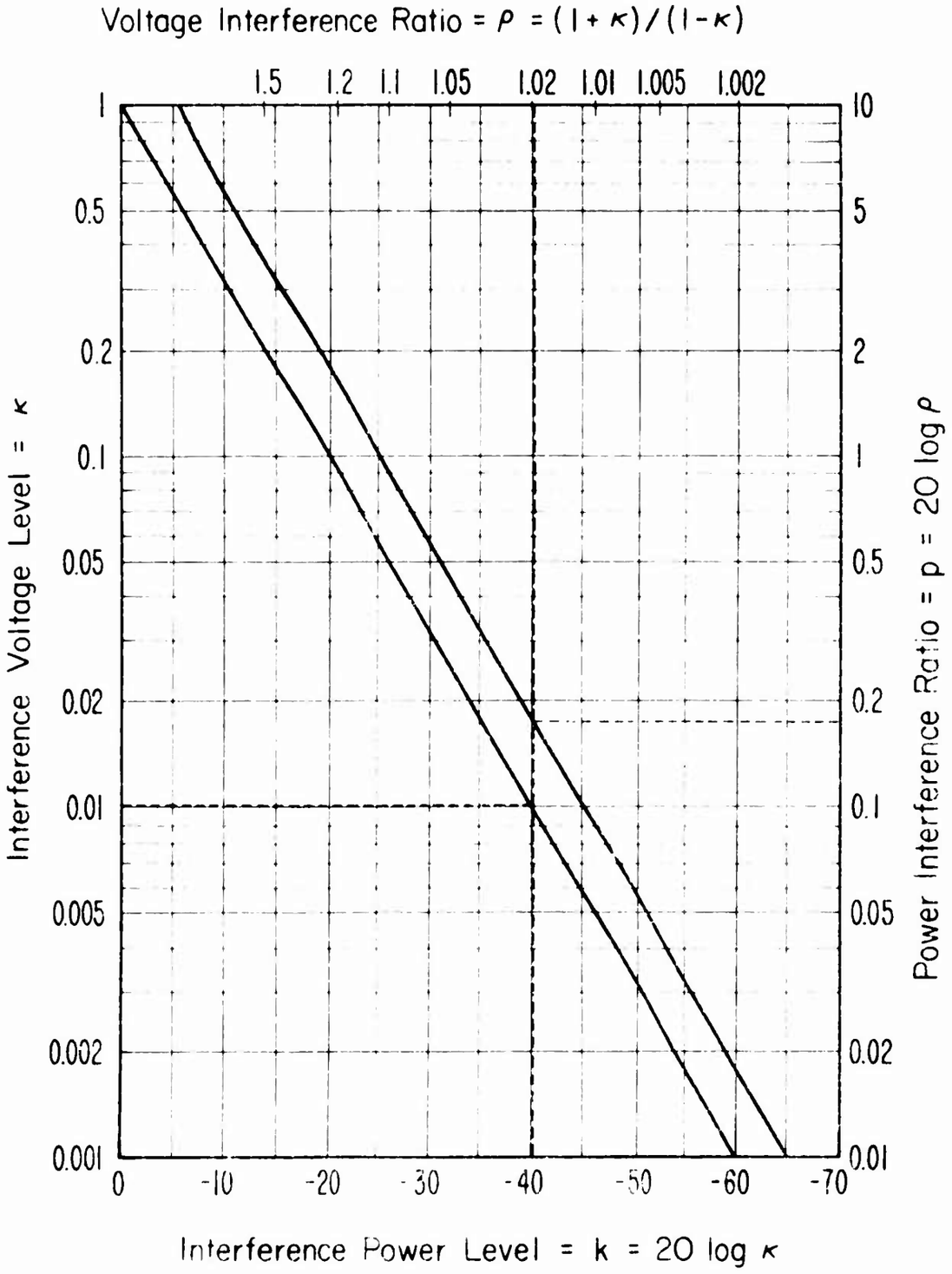

Fig. 3. Graph of Multipath Interference Parameters

The power interference ratio (PIR) is a particularly useful concept. For the moment, suppose that there is only one MPI component. Then, if the antenna is moved or if the generator frequency is swept by amounts that are large enough to cause reversals in the relative phase δ, the peak-to-peak variations in the decibel value of the received power will be equal to the power interference ratio p. That is,

$$10 \log\left(\frac{P_L \text{ max}}{P_L \text{ min}}\right) = p. \tag{14}$$

If a number of small interference components are present, then

$$10 \log\left(\frac{P_L \text{ max}}{P_L \text{ min}}\right) \approx p_1 + p_2 + p_3 + \ldots \tag{15}$$

with less than 0.04 dB error if the sum of the p's is less than 3 dB. Of course, the power perturbations are not perfectly symmetrical about P_{L0} ; but if the sum of the p's is less than 1.0 dB

$$10 \log\left(\frac{P_L \text{ max}}{P_{L0}}\right) \approx \tfrac{1}{2}(p_1 + p_2 + p_3 + \ldots) \tag{16}$$

$$10 \log\left(\frac{P_L \text{ min}}{P_{L0}}\right) \approx -\tfrac{1}{2}(p_1 + p_2 + p_3 + \ldots) \tag{17}$$

with less than 0.016 dB error (less than 0.005 dB error if the sum of the p's is less than 0.5 dB).

Obviously, p/2 provides an estimate of the uncertainty (expressed in decibels) in the received power associated with an interference component of known or estimated magnitude but unknown phase. For instance, if the estimated interference power level k is -40 dB for a MPI component, then the corresponding uncertainty in the received power is approximately $\pm$ 0.1 dB.

The maximum possible uncertainty in the received power due to a number of small MPI components is estimated easily from (16) and (17).

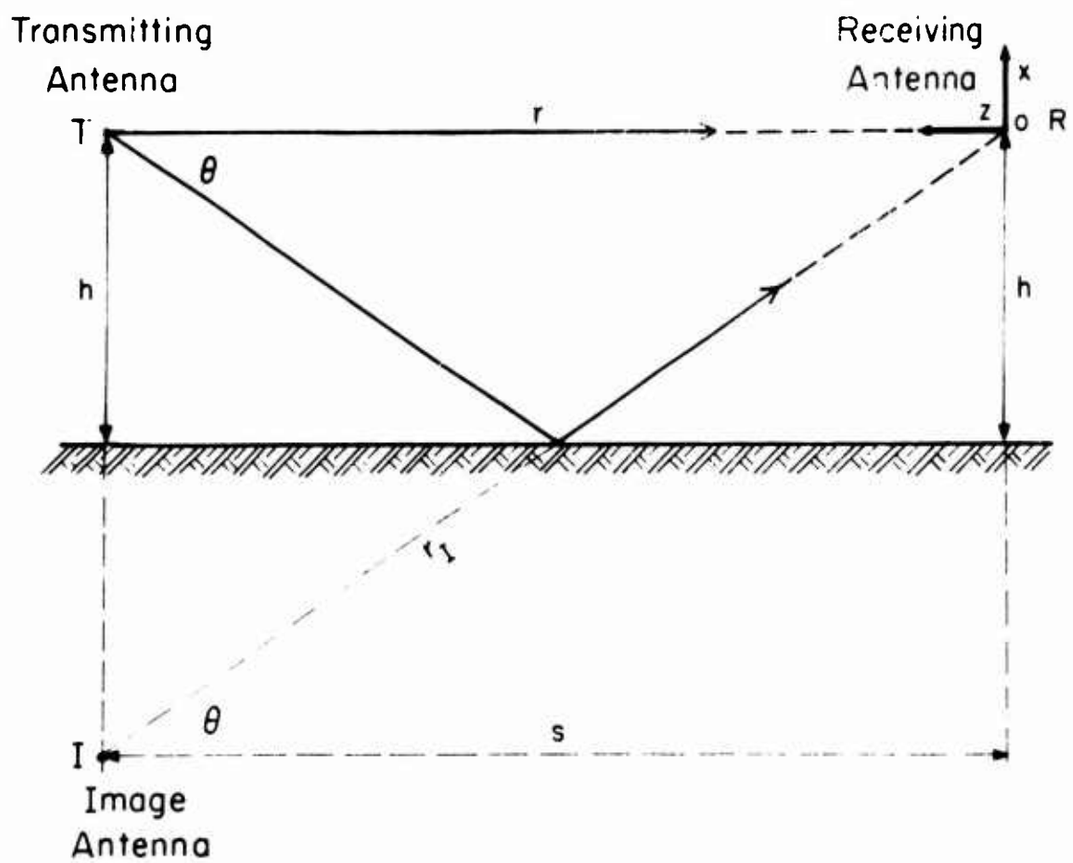

Fig. 3. Simple antenna range showing multipath interference from a reflection image of the transmitting antenna. Receiver movements used to evaluate multipath interference are related by rectangular coordinates located as shown.

4.4 Estimating the Effects of Multipath Interference.

When designing or evaluating antenna measurements, it is important to be able to make rough estimates of the effects of MPI. The following formulas, which emphasize simplicity rather than accuracy, are very useful for estimating the effects of MPI from the two most common sources of multipath components (see Fig. 3, which also serves to define several symbols soon to be used): (1) a "reflection"

image, (2) the "back-and-forth" (mutual) scattering from receiver-to-transmitter-to-receiver. As a rule, only one or the other of these two MPI components will be significant for a given gain measurement. If near-zone corrections can be determined for the horns, they can be located closely enough so that only the mutual-scattering component will be significant (this is usually true even if the gain measurements are made in a small room or small anechoic chamber). If the gain measurements must be made in the far-zone, an outside site will nearly always be necessary for accurate measurements; and a reflection from the ground will usually be the only significant MPI component. (Note: Scattering from antenna towers or from objects behind the transmitter and receiver can usually be made very small by using high-performance radiation-absorbing materials, which have very low "back-scatter" for perpendicular incidence.)

Estimating the interference power level k_I for the image component is straightforward:[16]

$$k_I = (\text{transmitter pattern level, in dB, for } \theta) + (\text{receiver pattern level, in dB, for } \theta) - (\text{surface loss, in dB, for } \theta) + 10 \log\left(\frac{r}{r_I}\right). \qquad (18)$$

The surface loss is difficult to estimate accurately[16], but this loss is usually not very important for horn gain measurements because the surface loss term will usually be small compared to the pattern levels of the antennas. Unless the surface is a radiation-absorbing material with known loss for the angle θ, zero surface loss should be assumed for horizontal polarization for all values of θ; but, except for surfaces with greater conductivity than average ground, a loss of at least 6 dB can be assumed for vertical polarization if θ is larger than 10 degrees.[16]

If the receiving antenna is moved from the origin 0 along the x-axis, it is easy to show[3] that the increment Δx required to cause one complete perturbation cycle for the image component is given approximately by

$$\Delta x \approx \frac{\lambda}{2} \left(\frac{s}{h}\right), \tag{19}$$

For movements along the other two axes, the corresponding increments are given by

$$\Delta y \approx (s\lambda)^{\frac{1}{2}} \left(\frac{s}{h}\right), \tag{20}$$

and

$$\Delta z \approx \frac{\lambda}{2} \left(\frac{s}{h}\right)^2 . \tag{21}$$

Equations (19), (20), and (21) underestimate the movements required for one perturbation cycle. They are correct to within about 15 percent if $s > 4h$ and if the total movement (x, y, or z) is less than $\frac{1}{2}h$; and they are correct to within about 50 percent if $s > 2h$ and x, y, or $z < \frac{1}{2}h$. (When s is about 2h or less, the directivity of most horns is great enough that the interference from the surface will not be important.)

Inspection of (19), (20), and (21) shows that it is not practical to use movements along the y-axis to produce perturbations in P_L corresponding to the image component. Obviously, x-axis movements are most efficient; but, nevertheless, it is usually desirable to use z-axis movements so that perturbations will be produced simultaneously for the MPI caused by mutual scattering or by multiple scattering between the antennas and the antenna mounts and towers. Except, perhaps, when

making gain measurements in the far-zone, where s is commonly much larger than h, z-axis movements will always be most satisfactory.

The successive scatterings between the two antennas will produce a series of multipath components, but only the first term of this series is important for separation distances larger than a^2/λ. By making some gross assumptions, it can be shown[3] that for identical horns the power interference ratio p_m for the mutual scattering component can be estimated from

$$p_m \approx \frac{1}{\rho^2} \tag{22}$$

where $\rho = \frac{r\lambda}{a^2}$. ($\rho$ is the separation distance in "Rayleigh" lengths.) For the case of non-identical horns, it can be shown that

$$p_m \approx \frac{1}{\rho_1 \rho_2} \tag{23}$$

where $\rho_1 = \frac{r\lambda}{a_1^2}$ and $\rho_2 = \frac{r\lambda}{a_2^2}$.† (Approximations (22) and (23) assume "normal" conditions, that is: matched antenna polarizations, antennas aligned for maximum power transfer, and small Γ_G, Γ_T, Γ_R, and Γ_L.) If one of the antennas is moved along the z-axis, it is evident that the perturbations in P_L for the mutual MPI will have a period of $\lambda/2$. Only a crude estimate of the "worst-case" peak-to-peak (dB) perturbations is provided by (22) or (23). For some frequencies p_m may actually be nearly zero, and for any frequency p_m is very unlikely to be larger than the estimate given by (22) or (23). Thus, for identical antennas the power variations due to mutual MPI can be expected to be no larger than ± 0.5 dB at a separation of only a^3/λ.

† Equations (22) and (23) are not limited to horn antennas. They can also be used to make rough estimates of the "worst-case" mutual MPI between any aperture antennas whose back-scatter is given approximately by $1/3\, A_p G S$, where A_p is the physical area of the antenna's perture, G is antenna's gain, and S is the power density of the incident field.

For swept-frequency gain measurements, it is important to be able to estimate the change in frequency required to produce a perturbation cycle for a given MPI component. Let $\mathcal{D}$ be the difference in path-length between the direct component and the indirect component and let λ_1 be the larger wavelength and λ_2 be the smaller wavelength corresponding to the terminal frequencies for a frequency sweep. Then the number of perturbation cycles produced by the frequency sweep is given by

$$\frac{\mathcal{D}}{\lambda_2} - \frac{\mathcal{D}}{\lambda_1} = (f_2 - f_1)(10^9)\,\frac{\mathcal{D}}{c} \qquad (24)$$

where the terminal frequencies f_2 and f_1 are in units of GHz and c is the speed of electromagnetic radiation. Therefore, the frequency increment Δf in GHz required to produce one perturbation cycle is

$$\Delta f = \frac{c}{\mathcal{D}\,(10^9)} \qquad (25)$$

Then it is easy to show that Δf for the surface MPI component is given approximately by

$$\Delta f_1 \approx \frac{3}{20s}\left(\frac{s}{h}\right)^2 , \qquad (26)$$

where s is in meters. For the mutual MPI component, $\mathcal{D} \approx 2s$ and Δf is given approximately by

$$\Delta f_m \approx \frac{3}{20s} , \qquad (27)$$

where s is in meters. Equation (26) is accurate to within about 20 percent if $s > 2h$. The accuracy of (27) is limited by the fact that the scattering from a horn does not occur at any definite place within the horn. The scattering from pyramidal horns appears to occur near the throat rather than at the aperture (see Section A1.5), and the accuracy of (27) for these horns can be improved somewhat by using the distance between the throats of the horns for s.

4.5 Multipath Interference When Measuring the Reflection Coefficients of Horns.

It is necessary, of course, that "free-space" conditions exist when measuring the reflection coefficients, Γ_T and Γ_R, of the antennas. Best practice is to point the antenna skyward or, which is usually easier, to point the antenna into a large outside space that is free of objects that could cause significant back-scatter. However, an adequate approximation to free-space can usually be obtained, for horn antennas at least, by pointing the horn perpendicularly at a wall of high-performance radiation-absorbing material. The horn should be at least a^2/λ from the material, and the material should intercept at least the entire main lobe of the radiation pattern of the horn. Typically, this arrangement will limit the MPI error when measuring $|\Gamma|$ for a horn antenna to less than ± 0.01. This error can be experimentally evaluated (and to some extent averaged out) by moving the horn or absorbing wall so as to introduce phase shifts in the "received" voltage waves from the back-scattered fields.

4.6 Energy Absorbed by the Generator from Back-Scattered Fields.

Particularly when making gain measurements in the near-zone, the generator may absorb considerable energy from back-scattered fields. Obviously, the field back-scattered to the transmitter from the receiver is stronger than the field re-scattered to the receiver from the transmitter. Insofar as the generator is stable, this event will not affect the gain measurement. However, if the output of the generator is a leveling coupler, some fraction of the "received" voltage waves from the back-scattered fields will appear at the leveling detector because of the finite directivity of the coupler. This will cause a corresponding change, usually small, in the power output of the generator. Consequently, as the frequency is swept or as antenna movements are made to produce perturbations in the load power, perturbations will also be produced in the

power output of the generator. Therefore, to some extent, the perturbations in the load power will be due to these generator-power perturbations. In averaging out the perturbations in the load power, the effect of these generator-power perturbations on the gain measurement is eliminated to about the same degree that the MPI perturbations in the load power are eliminated by this averaging process. Even so, these perturbations in the generator power are undesirable because they add to the complexity of the total perturbations in the load power and this added complexity will increase the uncertainty of the averaging process. It is obviously bad practice to use a leveling coupler for the output component of the generator unless the coupler has high directivity (say 30 dB or more). If a low-directivity coupler is used for leveling, an attenuator or isolator should be added to the output port of the coupler to provide a more stable generator.

In effect, the back-scattered fields change the reflection coefficient of the transmitting antenna. The effective reflection coefficient of the transmitting antenna can be written as

$$\Gamma_{Te} = \Gamma_{T0} + \Gamma_{T1} + \Gamma_{T2} + \cdots \tag{28}$$

where Γ_{T0} is the reflection coefficient of the antenna when transmitting into free-space and Γ_{T1}, Γ_{T2}, etc. are the additional components of the effective reflection coefficient due to each of the voltage waves "received" from the corresponding back-scattered field. Typically, the magnitude of these additional components will be less than 0.01 except for the component Γ_{Tm} due to the direct back-scatter from the receiving horn. By the same procedure used to obtain (22) and (23), it can be shown that a rough "worst-case" estimate of $|\Gamma_{Tm}|$ is given by

$$|\Gamma_{Tm}| \approx \frac{1}{8\pi_1\pi_2} \tag{29}$$

with the same conditions that were stated for (22) and (23). For identical antennas separated by a^2/λ, $|\Gamma_{T2}| \approx .1$, which may easily be larger than $|\Gamma_{T0}|$.

4.7 Multipath Interference When Aligning the Antennas.

If the antennas are aligned by "peaking" the received power, multipath interference components can cause significant errors in the alignment. This is true for both the polarization alignment and the radiation axis alignment.[16] Because of their simple geometry, horn antennas can easily be aligned geometricaly to avoid this source of error. (Of course, if the horns are not accurately constructed then the radiation axis may not coincide with the geometric axis.)

Section A3 contains an illustration of some errors that could occur due to the mutual MPI if the horns are aligned by peaking the received power.

5. Summary and Conclusions.

The insertion-loss method of measuring absolute gain has been considered to be basically the same as a waveguide insertion-loss measurement but with a number of additional sources of uncertainty. Referring to Page 4, the additional uncertainties derive from conditions 1), 3), and 4). The uncertainties that derive from conditions 2) and the instrument uncertainties that result from measuring the quantities in (1) are common to any insertion-loss measurement, and these uncertainties were considered to be well-known and were not discussed in detail.

In the error analysis some of the conditions for equation ignored because it is felt that they are usually automatically satisfied to a high degree, with certain restrictions (see pages 4 and 5), and would not cause errors larger than 0.01 dB. The conditions for "infinite" antenna separation, free-space transmission, and matched polarizations were removed by writing equation (3). The only important conditions for (3) are: (a) ideal waveguide leads and connectors, (b) stable generator and load, and (c) single sinusoidal frequency. These conditions are common to any insertion-loss measurement; and by using precision connectors, "padding" the generator and load well, and using high purity RF sources or appropriate RF filters, the uncertainties due to conditions (a), (b), and (c) can be made very small.

From the measurements desribed in Section A1.4 and the improvements discussed in Section A1.5.3, it is concluded that absolute gain measurements for most pyramidal horn antennas can be made in a small indoor range (about 3 x 3 x 3 meters) on a swept frequency basis to within ±0.1 dB uncertainty limits.† In fact, later measurements have confirmed this statement for "NRL" [12] horns that operate above 2.6 GHz. For lower frequency "NRL" horns, a "two-story" high room, or an outside range, would be necessary to achieve this degree of accuracy because of the relatively low directivity of these horns.

† To achieve this degree of accuracy for horns with coaxial waveguide leads, it would probably be necessary to use precision coaxial connectors.

A1. Examples of Horn-Gain Measurements.

A1.1 Description of the Antenna Range.

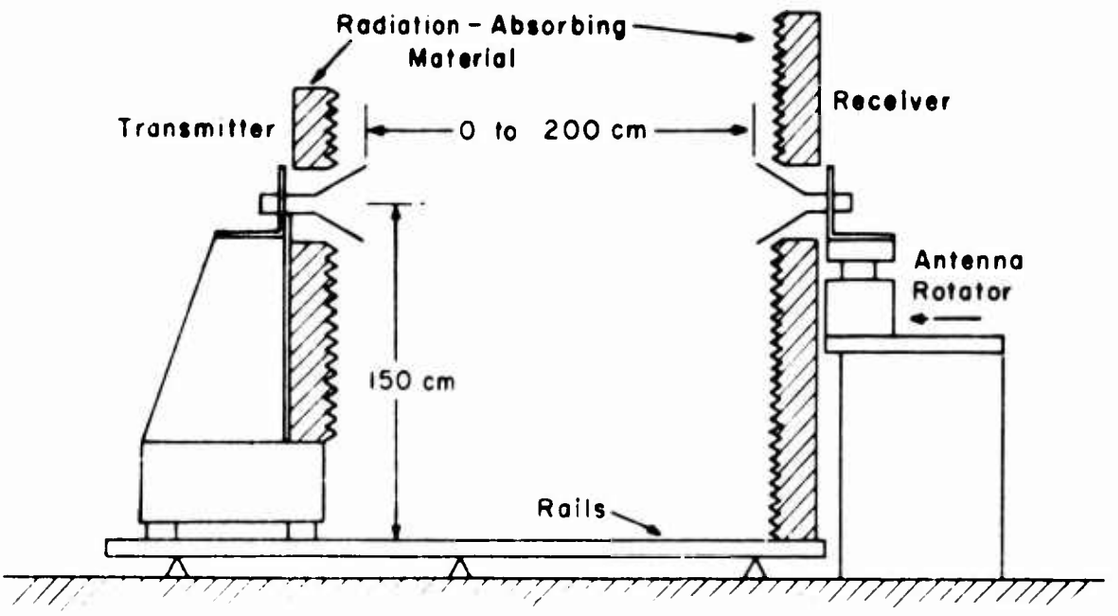

Fig. 4. Antenna Range.

The antenna range consisted of the equipment shown in Fig. 4. The transmitter pedestal slides on plastic blocks curved to fit the rails, which are round aluminum tubing. The radiation-absorbing material extends about 1 meter on each side of the receiver, and it extends about 0.3 meter on each side of the transmitter to completely cover the upper section of the pedestal. This equipment was located in an ordinary laboratory space with a ceiling height of about 3.5 meters. The space between the transmitter and receiver was open to a distance of about 1.5 meters or more in all directions perpendicular to the transmission axis, and the space

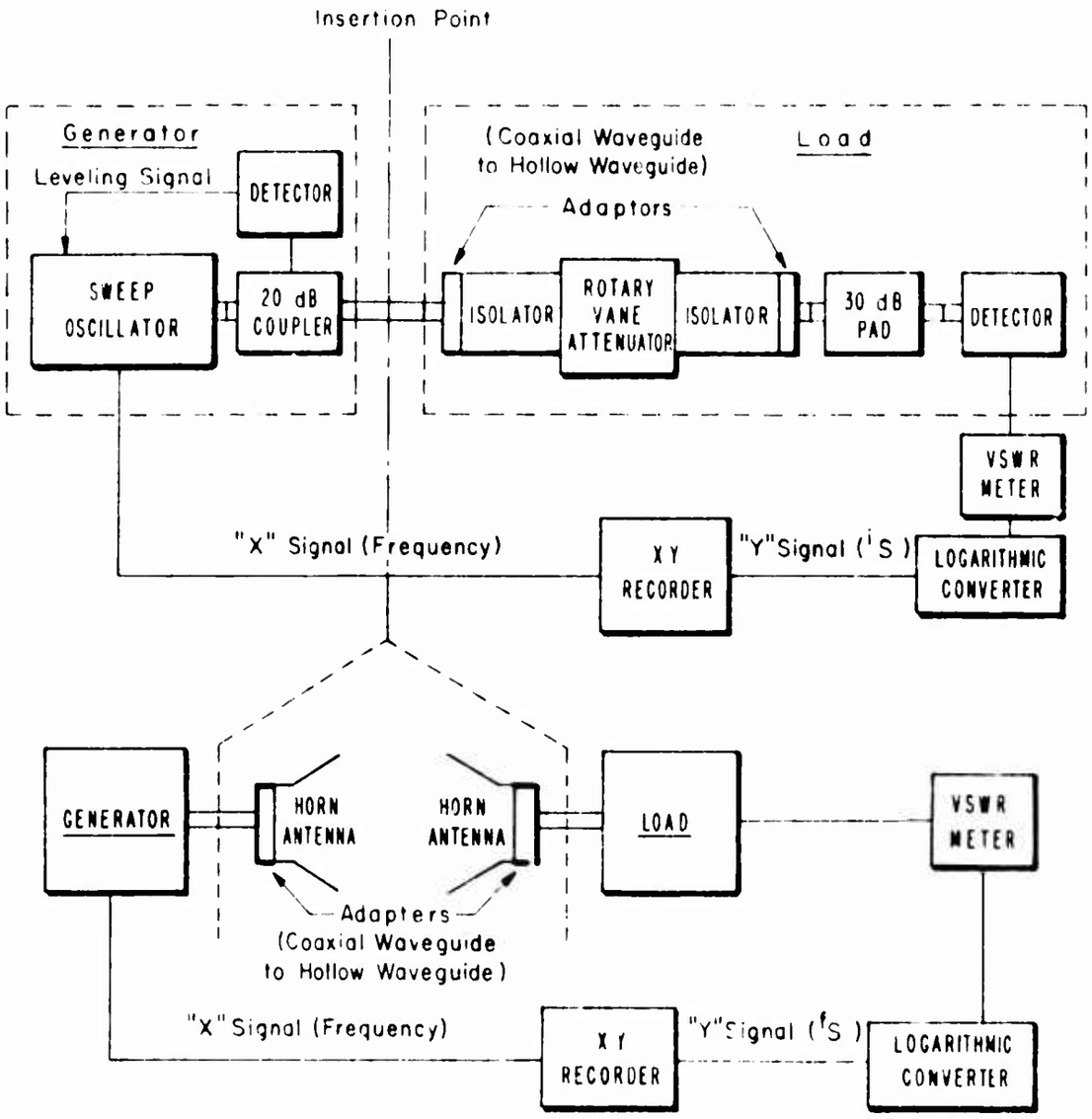

Fig. 5. Electronic and Waveguide Equipment.

behind the transmitter was open for a distance of about 2 meters. No radiation-absorbing material was used other than that shown in Fig. 4 despite the fact that the surrounding laboratory space was full of the usual clutter (metal cabinets, benches, equipment racks, lighting fixtures, etc.).

Even though the rails are quite straight and parallel, the distances between the plastic skids on the pedestal are fairly small so that there is a definite possibility of significant tilt as the pedestal is moved along the rails. The angle of this tilt was measured to be much less than 0.1 degree by placing sensitive levels on top of the pedestal and moving the pedestal along the rails.

A1.2 Swept-Frequency Horn Gain Measurement Using Coaxial-Waveguide Components.

A1.2.1 Description and Arrangement of the Electronic and Waveguide Equipment.

The electronic and waveguide equipment used is shown in Fig. 5. The microwave signal from the sweep oscillator was amplitude modulated (square-wave) at 1 kHz. Coaxial-waveguide components were used for the generator and load except for the rotary-vane attenuator and the hollow-waveguide components used to incorporate the rotary-vane attenuator into the load. All of the coaxial-waveguide components were equipped with type N connectors. The waveguide ports of the horns were female-N connectors and the waveguide ports of the generator and load were male-N connectors. The "initial" or "direct" coupling between the generator and load was provided by a 3 cm long male-to-male adapter.

For reasons that will be discussed in Section A1.5, all of the waveguide components were connected directly together (except for the connection between the sweep oscillator and the leveling coupler). A 3 meter length of coaxial waveguide was used between the sweep oscillator and the leveling coupler so that the sweep oscillator, along with the VSWR

meter, log converter, and X-Y recorder, could be located where this equipment and the operator would be outside of the main lobes of the antenna patterns.

The rotary-vane attenuator, with the isolators and waveguide adapters attached, had been previously calibrated so that the power level at the detector could be changed by accurately known amounts as needed during the insertion-loss measurement.

A1.2.2 Procedure.

Two identical pyramidal horns† (commercial versions of the "NRL" 6 cm band horn)[12] were mounted as shown in Fig. 4; and the aperture of the transmitting horn was aligned so that it was perpendicular to the direction of movement of the pedestal. The transmitter pedestal was slid to the receiver end of the range, and the aperture of the receiving horn was aligned so that it coincided as closely as possible with the aperture of the transmitting horn. The pedestal was slid back until the apertures were separated by 100 cm (roughly a^2/λ) to complete the orientation of the antennas.

The generator and load were coupled by means of the 3 cm long adapter, and the Y-gain and Y-zero controls on the X-Y recorder and the gain control on the VSWR meter were adjusted so that "full scale" (10 major divisions) on the recorder paper corresponded to "full scale" (10 dB) on the VSWR meter. To obtain a more accurate calibration of the Y-axis, the Y-axis controls were adjusted slightly so that a previously measured 10.00 ± 0.05 dB step on the range switch of the meter gave 10 major divisions of deflection on the Y-axis. This completed the calibration of the Y-axis. The X-gain and X-zero controls on the recorder were

† The physical identity of these two horns had been checked by carefully comparing their physical dimensions. Small differences were evident in their dimensions, but the corresponding differences in gain were estimated to be less than ± 0.02 dB. This estimate was based on the design formulas for these horns contained in reference 12.

adjusted so that a sweep of 4.0 to 6.0 GHz (as indicated by the frequency dial of the sweep oscillator) corresponded to 0 to 10 major divisions on the X-axis of the recorder paper. A cavity-type wavemeter was momentarily inserted between the generator and load, and the accuracy of the X-axis was measured to be within ±20 MHz to complete the calibration of the X-axis.

Adjustments were made in the power level from the sweep oscillator and the gain of the leveling amplifier to obtain a smooth load power curve for a sweep of 4.0 to 6.0 GHz. The power stability was observed for about an hour and it was noted that room temperature variations caused changes of about ± 0.1 dB in the indicated load power level.

The rotary-vane attenuator was set to a dial reading of 15 dB, and pads (totaling 30 dB) were added between the attenuator-isolator combination and the detector so that the signal from the detector was just large enough to give a "quiet" trace on the X-Y recorder (about ± 0.01 dB "jitter"). (This particular crystal-meter combination had been previously calibrated, at room temperature, so that the deviations from "square-law" response of the crystal were approximately known as a function of the power level at the detector. This data showed that the deviation from square-law response was very small for the power level then set at the detector. For power changes of plus or minus a few dB, the measured power change would be numerically smaller then the actual change by 0.005 ± 0.003 dB. Therefore, after the transmission path was inserted, the rotary-vane attenuator could be adjusted to give approximately the same power level at the detector and small deviations from this power level could be accurately read from the VSWR meter or X-Y recorder.) The calibrations of the X and Y axes were checked, and no recalibration of the recorder was required. This completed the alignment and calibration of the equipment.

With the generator and load directly connected, the initial load power signal was recorded (see Fig. 6). As a result of the calibration procedure, the recorder signal ${}^{i}S$ is given by

$$ {}^{i}S = 10 \log ({}^{i}C\,{}^{i}P_{L}), \tag{30} $$

where ${}^{i}C$ is a conversion factor determined by, among other things, the various instrument control settings and the oscillator frequency. Within the linearities and stabilities of the measurement system and since the rotary-vane attenuator is the only control adjusted during the insertion-loss measurement, the conversion factor is a function only of the oscillator frequency and the rotary vane attenuator setting. The generator and load were then connected to the two horns; the rotary-vane attenuator was adjusted to an integral setting such that the final signal was within 2 dB of the initial signal; and the final signal ${}^{f}S$ was recorded. The final signal is related to the final load power by

$$ {}^{f}S = 10 \log ({}^{f}C\,{}^{f}P_{L}), \tag{31} $$

where ${}^{f}C$ differs from ${}^{i}C$ only by the change in the setting of the rotary-vane attenuator. Since the initial setting of the rotary-vane attenuator was 15 dB, the final setting was 5 dB, and the calibration uncertainty for the 5 dB to 15 dB step of the attenuator was ± 0.1 dB throughout the 4.0 GHz to 6.0 GHz range,

$$ {}^{f}S = 10 \log ({}^{i}C\,{}^{f}P_{L}) + (10.0 \pm 0.1)\ \text{dB}. \tag{32} $$

Therefore, by combining (32) and (30),

$$10 \log\left(\frac{{}^{f}P_{L}}{{}^{i}P_{L}}\right) = ({}^{f}S - {}^{i}S) - (10.0 \pm 0.1)\ \text{dB}. \qquad (33)$$

Without changing the rotary-vane attenuator setting, the transmitter was slid back and two more "final" load power signals were recorded, one for a separation of 150 cm and the other for a separation of 200 cm. Then the generator and load were re-coupled and another "initial" load power signal was recorded to provide a "check" on the drift of the system. Since less than 10 minutes had elapsed between the two recordings of the "initial" load power signal, it is not surprising that the two recordings were within ± 0.02 dB of their averaged values, though it is possible that the drift was larger and was cancelled by a difference in the connector and adapter losses of the original and later couplings of the generator and load.

To provide estimates of the uncertainty limits for the mechanical and positional stabilities of the generator and load and for the repeatability of the connectors, the generator and load were coupled together about ten times, rotating the connectors and the adapter between each coupling. For each coupling, the leveling coupler and load combination was moved and twisted while observing the load power signal. The maximum changes that could be produced in the load power signal by these procedures were within ± 0.1 dB. This relatively large variation is attributed to the fact that the leveling coupler was an old model with rather poor connectors.

So that estimates could be made for the uncertainties in the alignment of the direction angles of the horns, the E-plane and H-plane radiation patterns of the horns were measured over a range of about 5 degrees from the radiation axis. (See Section A3 for the results and discussion of the E-plane pattern measurements.)

Because all of the components of the generator and load are broad-band, the spectral width of the fundamental frequency output of the oscillator is not critical. However, harmonic frequency outputs from the oscillator could cause substantial errors. The level of the first harmonic frequency output of the oscillator was measured to be about 50 dB below the fundamental for fundamental frequencies of 4.0, 4.2, and 4.4 GHz and more than 60 dB below the fundamental for the other fundamental frequencies.

A1.2.3 Determining the Free-Space Insertion-Loss.

The free-space load power ${}^{f}P_{L0}$ could be determined by measuring the conversion factor ${}^{i}C$ (or ${}^{f}C$), but this is not necessary since only the ratio of the initial and final load powers is needed and the conversion factor of the metering equipment cancels out of this ratio. Since the perturbations in ${}^{f}S$ that result from multipath interference are equal to the corresponding perturbations in the decibel value of ${}^{f}P_{L}$,

$$ {}^{f}S_{0} = 10 \log ({}^{f}C\,{}^{f}P_{L0}) = 10 \log ({}^{i}C\,{}^{f}P_{L0}) - (10.0 \pm 0.1) \qquad (34) $$

and

$$ 10 \log \left(\frac{{}^{f}P_{L0}}{{}^{i}P_{L}} \right) = ({}^{f}S_{0} - {}^{i}S) - (10.0 \pm 0.1) \qquad (35) $$

where ${}^{f}S_{0}$ is the final load power signal with the multipath interference perturbations averaged out and is the signal that would result from free-space power transmission.

Unfortunately, the process of averaging out the MPI perturbations is not a straight-forward procedure. There is the annoying possibility that the gain function of the horns will have periodic variations with respect to frequency, and a serious error could result if the corresponding variations in ${}^{f}S$ were mistaken for MPI perturbations and were averaged out. In fact, such periodic variations in the gain functions of small horns have been strongly suggested by previous horn-gain

measurements[12, 17] and are also strongly suggested by the curves of Fig. 6. By comparing the recordings of the final load power signal for the three separation distances, it is evident that the large, long-period variations in ^{f}S do not change as the separation distance is changed by large amounts. This means that these variations are not due to MPI and should not be averaged out. Since the small, short-period variations in ^{f}S are dependent on separation distance, they represent perturbations caused by MPI and they are averaged out to obtain $^{f}S_0$, which is represented by the dashed lines in Fig. 6.

Considering this gain measurement alone, the large long-period variations in $^{f}S_0$ cannot be definitely attributed to the gain function of the horns. Because the mismatch function was not evaluated for this measurement, the possibility that the variations in question are due to mismatch cannot be excluded. However, from previous gain measurements on these horns in which the mismatch losses were completely evaluated and also from the more accurate gain measurements for these horns presented in Section A1.3, it is known that these variations are primarily due to the gain function of the horns.

Even though it is good practice to record ^{f}S for several separation distances (since this additional information is useful in establishing which variations in the received power are due to MPI), it may not always be convenient or feasible to do this. For a well-designed gain measurement, however, the periods of the significant MPI components will be calculated and the measurement will be designed accordingly so that there will be no confusion between the gain variations and the MPI perturbations. Then it will not be necessary to record ^{f}S for more than one separation distance. (See the discussion in Section A1.5).

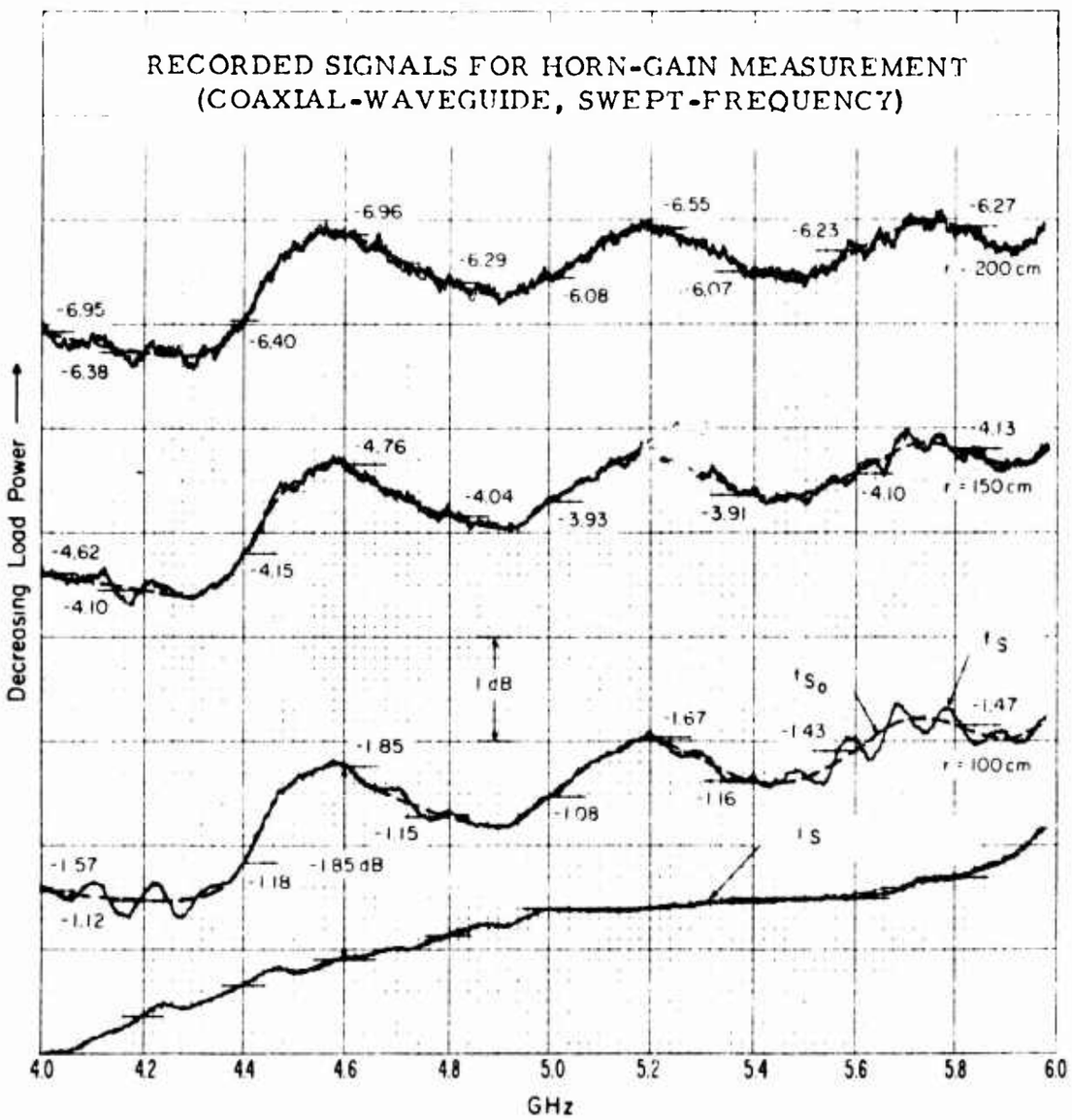

Fig. 6. Recorded Signals for Horn-Gain Measurement (Coaxial-Waveguide, Swept-Frequency)

Frequency GHz	Wavelength cm.	5 log N	5 log M	10 log (4πr) −5 log DR	−10 log λ	$5 \log\left(\frac{P_{r,\theta}}{P_t}\right)$ plus uncertainties for conditions (a), (b), (c)	G
4.00	7.49	.40 ± .04	0.0 ± .60	$32.75 \begin{smallmatrix}+.02\\-.00\end{smallmatrix}$	-8.75 ± .02	-7.32 ± .27	17.08 ± 1.00
4.20	7.14	.44 ± .04			-8.54	-7.06	17.59
4.40	6.81	.48 ± .05			-8.33	-7.08	17.82
4.60	6.52	.51 ± .05			-8.14	-7.39	17.73
4.80	6.25	.56 ± .06			-7.96	-7.03	18.32
5.00	6.00	.60 ± .06			-7.78	-6.97	18.60
5.20	5.77	.64 ± .06			-7.61	-7.23	18.55
5.40	5.55	.69 ± .07			-7.44	-6.96	19.04
5.60	5.35	.74 ± .07			-7.28	-7.06	19.15
5.80	5.17	.78 ± .08			-7.13	-7.07	19.33

Fig. 7. Results of Gain Computation (Coaxial Waveguide, Swept-Frequency).

A1.2.4 Computing the Gain and Assigning the Uncertainty Limits.

From the footnote on page 34, the gain of each horn is within ± 0.01 dB of $\sqrt{G_T G_R}$, and it will be assumed that the gains are identical. Then, from (3),

$$10 \log G = 5 \log N + 5 \log M + \left[10 \log (4\pi r) - 5 \log (DR)\right] - 10 \log \lambda + 5 \log \left(\frac{{}^{f}P_{L0}}{{}^{f}P_{L}}\right) , \qquad (36)$$

where 5 log (DR) and 10 log (4πr) have been grouped together because these terms contain all of the orientation variables. Below, a sample gain computation and assignment of uncertainty limits for 4.0 GHz is made using ${}^{f}S_{0}$ data for the 150 cm separation distance. The results are shown in Fig. 7 along with the results for a number of other frequencies.

The near-zone correction, 5 log N, is given by Fig. 20 in Section A4. For 4.0 GHz and r = 150 cm and using the conservative estimate of ±10% for the uncertainty limits, 5 log N = 0.40 ± 0.04.

Since none of the quantities in the mismatch factor were measured, only estimates for the upper and lower bounds for 5 log M can be determined. From manufacturer's data on the waveguide components, it is estimated that a reasonable upper limit for $|\Gamma|$ for the generator†, load, and both horns is 0.2 for any frequency within the 4.0 GHz to 6.0 GHz range. A lower limit of zero is assumed for $|\Gamma|$ for each horn. Substituting $|\Gamma_T|_U = |\Gamma_R|_U = |\Gamma_G|_U = |\Gamma_L|_U = 0.2$ in (7), and substituting $|\Gamma_T|_\ell = |\Gamma_R|_\ell = 0$ and $|\Gamma_G|_U = |\Gamma_L|_U = 0.2$ in (8) gives 5 log M = 0.00 ± 0.60.

† It should be mentioned that, contrary to recommended practice, the leveling coupler used in this gain measurement did not have very high directivity. The minimum directivity of the coupler was only 20 dB. For this coupler, S_{22} was 0.08 or less, and (9) gives a maximum effective reflection coefficient magnitude of 0.18 for the generator port. Since low reflection coaxial-waveguide pads have a $|\Gamma|$ of less than 0.1 in the 4.0 to 6.0 GHz range, it would have been better practice to have added a low-reflection pad to the output of this leveling coupler. Also, a low-reflection pad should have been used to provide a better-matched input port for the load.

In assigning values and uncertainty limits to the orientation variables D, R, and r, it will be assumed that the values of D and R are one. (Since the antennas were aligned geometrically, the assumption that the value of D is one is equivalent to the assumption that the geometric and electromagnetic axes of each horn are the same. The assumption that the value of R is one is equivalent to the assumption that the horns have identical polarization parameters) From the measured patterns of the horns and estimating that the four direction angles (two for each horn) were all 0.0 ± 0.1 degree with respect to the common transmission axis, the power loss due to directional misalignment is estimated to be less than 0.04 dB. Then $5 \log D = 0.00 \begin{smallmatrix} + 0.00 \\ - 0.02 \end{smallmatrix}$. The uncertainty in the rotational alignment is also estimated to be less than ± 0.1 degree, and since R varies slowly with the rotation angle, no uncertainty is assigned to R. Then $5 \log R = 0.00 \pm 0.00$. The uncertainty in the 150 cm separation distance is within ±0.1 cm; and neglecting this small uncertainty, $10 \log 4\pi r = 32.75 \pm 0.00$. Therefore, $\left[10 \log (4\pi r) - 5 \log (DR)\right] = 32.75 \begin{smallmatrix} + 0.02 \\ - 0.00 \end{smallmatrix}$.

The uncertainty in the frequency is within ±20 MHz. This corresponds to an uncertainty of 0.5% in the 7.49 cm wavelength for 4.0 GHz (and somewhat less uncertainty for the other frequencies). Therefore, $10 \log \lambda = 8.75 \pm 0.02$.

A number of uncertainties are involved in determining $10 \log ({}^{r}P_{L} / {}^{i}P_{L})$, which is the negative of the insertion-loss. One of these uncertainties is the ± 0.1 dB uncertainty in the power-level change produced by the rotary-vane attenuator, and this uncertainty is included explicitly in (35). Estimates for the other uncertainties are as follows:

Uncertainty in determining ${}^fS_0$	-	± 0.10 dB
Uncertainty in $({}^fS_0 - {}^1S)$ due to the frequency uncertainty†	-	± 0.10 dB
Noise on ${}^1S$	-	± 0.02 dB
Y-axis calibration uncertainty	-	± 0.02 dB
Time and Temperature stability of the generator and load	-	± 0.05 dB

Also, from the approximately known deviation of the detector from square-law response, a small correction of -0.02 ± 0.01 dB is added to $({}^fS_0 - {}^1S)$. From Fig. 6, the value of $({}^fS_0 - {}^1S)$ is -4.62; therefore, $({}^fS_0 - {}^1S) = -4.64 \pm 0.30$ dB. Then, from (35), the negative of the insertion-loss is -14.64 ± 0.40; and 5 log $({}^fP_{L0}/{}^1P_L) = -7.32 \pm 0.20$.

The effects of violations of the conditions (see page 6) on (3) and (36) have not been well enough determined here to permit convincing estimates to be made for the corresponding uncertainties. Therefore, the following estimates are relatively subjective. Referring to page 37, a net uncertainty of ±0.1 dB in the measured insertion-loss is estimated for violations of conditions (a), ideal waveguide leads and connectors, and (b), stable generator and load. As noted on page 38, the spectral width of the fundamental frequency output of the oscillator is not critical, and no uncertainty is assigned for the finite spectrum width of the fundamental frequency. Spurious frequencies, other than the first harmonic, were not measured but are assumed to be negligible. The measured first harmonic levels could cause a few hundredths of a dB error in the measured insertion-loss only for the fundamental frequencies of 4.0, 4.2, and 4.4; and ± 0.04 dB is assigned for violations of (c), single sinusoidal frequency. Then the estimated uncertainty in the gain due to violations of (a), (b), and (c) is ± 0.07 dB.

† The uncertainty in $({}^fS_0 - {}^1S)$ due to the frequency uncertainty is determined mainly by the slope of ${}^fS_0$ and is actually much less than ± 0.1 for 4.0 GHz. The estimate of ± 0.1 dB is estimated to be the worst case for any frequency in the band.

As estimated above, all of the individual uncertainty limits, except the uncertainty limits for N, are worst-case limits that apply to any frequency in the band. Then, using the worst-case uncertainty limits for N of ±0.08 at 5.8 GHz, summing the individual limits, and rounding off the totals, the absolute uncertainty limits estimated for any frequency in the band are +1.00 dB and -1.00 dB. Because most of the individual uncertainties were conservatively estimated and because there are so many independent sources of uncertainty involved, these total uncertainty limits are considered to be unreasonably conservative. It is felt that a more reasonable estimate of the combined limits of uncertainty can be obtained by taking the root-sum square[†] of the individual uncertainty limits.[18,19] This procedure is complicated by the fact that the uncertainty limits stated for M are actually the sum of a number of independent uncertainties. For purposes of illustration, an approximation to the root-sum-squre of the individual uncertainty limits can be obtained by considering the uncertainty limits for 5 log M to be the sum of four independent uncertainties with limits of ±0.15 each and by grouping the other uncertainties to give four uncertainties of ±0.1 each. Then, the "root-sum-square uncertainty limits" for the gain values are approximately $\pm \left[4(0.15)^2 + 4(0.1)^2\right]^{\frac{1}{2}} = \pm 0.36$ dB. (A more detailed computation gives limits of +0.33 and -0.28). The gain values for this measurement do not differ by more than 0.25 dB from the corresponding values for the more accurate measurement described in Section A1.3.

[†] Technically, one should take the root-sum-square of the individual percentage limits of error and then convert this number to dB. But, for small individual limits of error, the root-sum-square of the individual dB limits provides a good approximation to the dB value of the root-sum-square of the individual percentage limits.

A1.3 Swept-Frequency Horn-Gain Measurement Using Hollow-Waveguide Components.

A1.3.1 Equipment.

Aside from using hollow-waveguide components in place of the coaxial-waveguide components and except as noted below, the equipment was the same as that shown in Fig. 5 and described in Section A1.2.1. For the hollow-waveguide measurement, the output component of the generator was a 10 dB, high-directivity directional coupler, and the input component of the load was the input isolator of the isolator-attenuator combination. The horns, with the coaxial-waveguide to hollow-waveguide adapters removed, were the same as those used previously.

A1.3.2 Procedure.

Except as noted below, the procedure was the same as that outlined in Section A1.2.2. For the hollow-waveguide-measurement, ice-packs were placed around both detectors for improved thermal stability. (By a simple procedure that need not be described here, it was established that there was no significant difference in the square-law response of the load detector at room temperature and at 0^{o} centigrade.) Also, the absorption "pips" produced by the cavity wavemeter used to calibrate the frequency axis were recorded at 200 MHz intervals (see Fig. 8), and the "free-space"[†] $|\Gamma|$'s for each horn[††] and for the load were measured for each of these frequencies. Other

---

† When measuring $|\Gamma_T|$ and $|\Gamma_R|$, the horns were pointed into a wall of radiation - absorbing material; and the distance to the absorbing wall was varied for each frequency to evaluate the effects of the back-scatter from the absorber. The back-scatter caused variations of less than 0.002 in the measured values of $|\Gamma_T|$ and $|\Gamma_R|$.

†† The reflection coefficients for these two horns differed by less than 0.01 in magnitude at these frequencies, but differences as large as 0.05 have been measured for X-band horns of nearly identical construction.

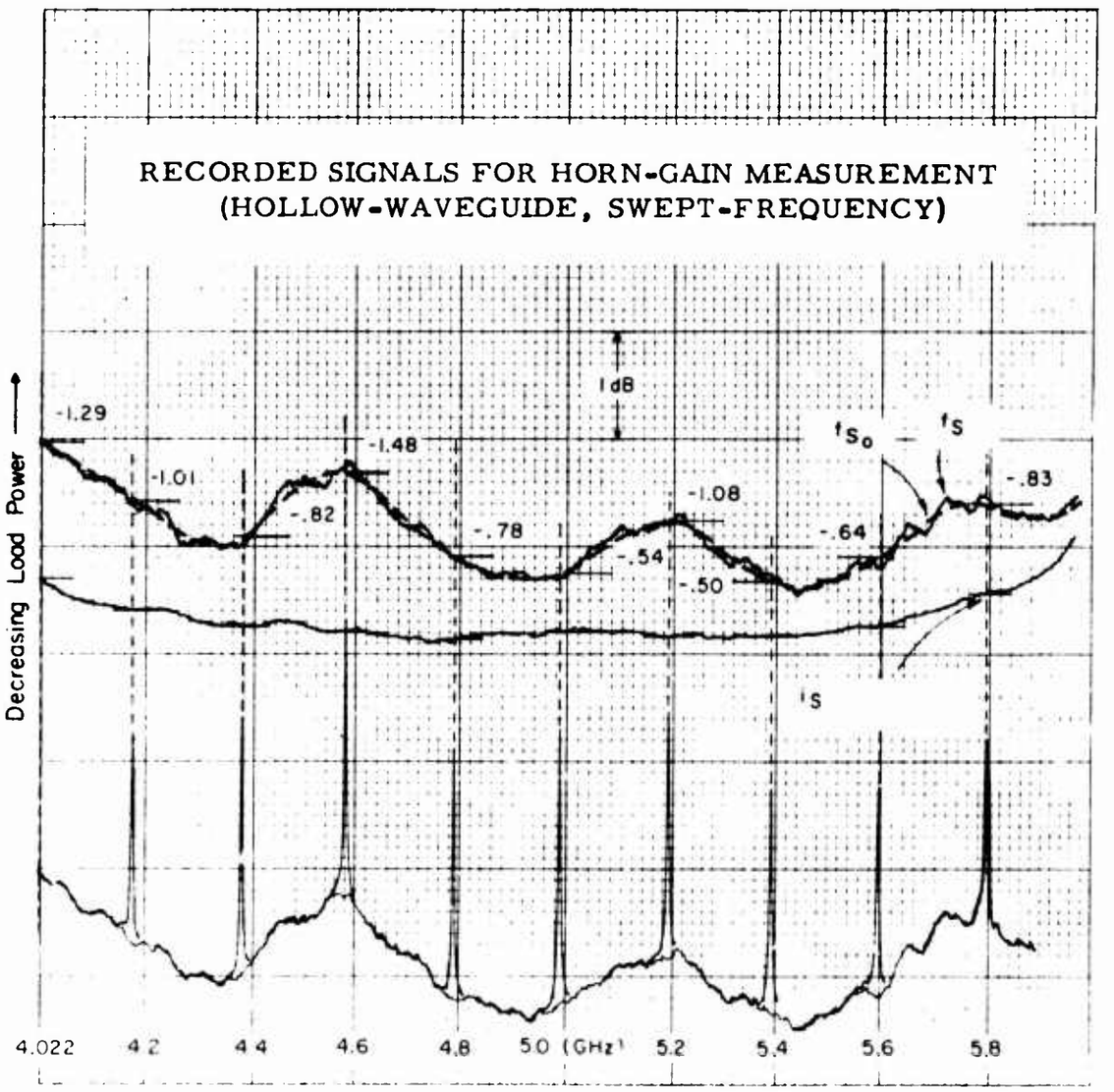

Fig. 8. Recorded Signals for Horn-Gain Measurement (Hollow-Waveguide, Swept-Frequency).

Frequency GHz	Wavelength cm.	5 log N	5 log M	10 log (4πr) -5 log DR	-10 log λ	$5 \log\left(\frac{{}^{t}P_{L_0}}{{}^{t}P_{L}}\right)$ plus uncertainties for conditions (a), (b), (c)	G
4.022	7.46	.40 ± .04	.01 ± .04	32.75 $^{+.02}_{-.00}$	-8.73 ± .00	-7.15 ± .16	17.28 ± .26
4.20	7.14	.44 ± .04	.01 ± .04		-8.54 ±	-7.00 ± .16	17.66 ± .26
4.40	6.81	.48 ± .05	.03 ± .07		-8.33 ±	-6.91 ± .16	18.02 ± .30
4.60	6.52	.51 ± .05	.01 ± .04		-8.14 ±	-7.24 ± .14	17.89 ± .25
4.80	6.25	.56 ± .06	.01 ± .03		-7.96 ±	-6.89 ± .14	18.47 ± .25
5.00	6.00	.60 ± .06	.03 ± .04		-7.78 ±	-6.77 ± .14	18.83 ± .26
5.20	5.77	.64 ± .06	.01 ± .03		-7.61 ±	-7.04 ± .14	18.75 ± .25
5.40	5.55	.69 ± .07	.01 ± .03		-7.44 ±	-6.75 ± .14	19.26 ± .26
5.60	5.35	.74 ± .07	.01 ± .04		-7.28 ±	-6.82 ± .14	19.40 ± .27
5.80	5.17	.78 ± .08	.01 ± .04		-7.13 ±	-6.92 ± .14	19.49 ± .28

Fig. 9. Results of Gain Computation (Hollow-Waveguide, Swept-Frequency).

differences in the procedure were that ${}^{f}S_0$ was recorded for only one separation distance (150 cm) and that a (13.0 ± 0.1) dB change in the rotary vane attenuator was used. It was not necessary to remeasure the patterns of the horns, of course; and the harmonic output of the generator was assumed to be the same as before.

A1.3.3 Computing the Gain and Assigning the Uncertainty Limits.

For the coaxial-waveguide measurement, the uncertainty limits for the gain were stated in terms of the worst-case limits for any frequency within the band because the fractional variation of the uncertainty limits with frequency was small. For the hollow-waveguide measurement, however, the fractional variation of the uncertainty limits is more important; and separate limits are stated for each frequency. Otherwise, the gain computation and the assignment of the uncertainty limits is essentially the same as for the coaxial-waveguide measurement. Equation (37) is used instead of (35) because a different "step" on the rotary-vane attenuator was used for the hollow-waveguide measurement:

$$10 \log \left(\frac{{}^{f}P_{L0}}{{}^{1}P_{L}} \right) = ({}^{f}S_0 - {}^{1}S) - (13.0 \pm 0.1) \qquad (37)$$

The sample computation below is for 5.0 GHz and the results are shown in Fig. 9.

From Fig. 20 in Section A4, the near-zone correction is $5 \log N = 6.00 \pm 0.06$, where the conservative estimate of ± 10% has been used for the limits.

All of the reflection coefficient magnitudes were small so that (6) can be used to compute the mismatch factor. For the leveling coupler used in this measurement, S_{22} was less than 0.025 and the directivity was greater than 40 dB for all frequencies. Therefore,

from (9), $|\Gamma_{ot}|$ was less than 0.035. The measured values for the other $|\Gamma|$'s were $|\Gamma_T| = |\Gamma_R| = 0.08 \pm 0.01$ and $|\Gamma_L| = 0.03 \pm 0.01$. The uncertainty limits for these $|\Gamma|$'s are small enough to be ignored, but this may not always be the case and then a little caution is necessary when substituting into (5) or (6). For purposes of illustration, the limits for the $|\Gamma|$'s will be assumed to be significant. Noting that the first bracket of (6) is a correction factor which will be uncertain to some extent because of the uncertainties in $|\Gamma_T|$ and $|\Gamma_R|$ and that the second term contributes only to the limits for M, the measured value and its bounds for $|\Gamma_T| = |\Gamma_R|$ should be substituted into the first term while only the upper bounds for the $|\Gamma|$'s should be substituted into the second term. Then,

$$M \approx \left[1+2\,(0.08 \pm 0.01)^2\right] \pm 2\left[(0.035)(0.09) + (0.09)(0.04) + (0.035)(0.04)\right]$$
$$= 1.0130 \pm 0.0032 \pm 0.0143 = 1.0130 \pm 0.0195$$

and $$5 \log M \approx 0.03 \pm 0.04.$$

The values and limits for the orientation variables, D.R. and r, are the same as before.

The uncertainty of 0.1% (0.004 dB) in the wavelength is negligible. Therefore, $-10 \log \lambda = -7.78 \pm 0.00$.

In addition to the 0.1 dB uncertainty in the power-level change produced by the rotary-vane attenuator, the uncertainties listed below are estimated for the negative of the insertion-loss, 10 log $({}^{f}P_{to}/{}^{i}P_{t})$. Referring to (37):

Uncertainty in determining ${}^fS_0$	-	± 0.10 dB
Uncertainty in (${}^fS_0$ - ${}^1S$) due to the frequency uncertainty	-	± 0.02
Noise on ${}^1S$	-	± 0.02
Y-axis calibration uncertainty	-	negligible
Time and temperature stability of generator and load	-	± 0.02
Deviation of the detector from "square-law" response	-	negligible

From Fig. 8 the value of (${}^fS_0$ - ${}^1S$) is - 0.54, therefore, (${}^fS_0$ - ${}^1S$) = - 0.54 ± 0.16. Then, from (37), the negative of the insertion-loss is - 13.54 ± 0.26; and 5 log (${}^fP_{L0}/{}^1P_L$) = -6.77 ± 0.13.

For violations of (a), ideal waveguide leads and connectors, and (b), stable generator and load, a net uncertainty of ± 0.02 dB is estimated in the measured insertion-loss. Uncertainties due to violations of (c), single sinusoidal frequency, are estimated to be negligible (see page 44). Therefore, ± 0.01 dB is assigned to the gain for violations of (a), (b), and (c).

Because most of the individual uncertainties were conservatively estimated and because there are so many independent sources of uncertainty involved, it is felt that a reasonable estimate of the combined uncertainty limits is obtained by taking the root-sum-squre of the individual uncertainty limits.[18,19] The gain values in Fig. 9 were compared to the corresponding values obtained from an earlier swept-frequency measurement performed for these same horns using a different range, a separation of about 100 cm, and different (hollow-waveguide) components for the generator and load. The largest disagreement between these two independent measurements was 0.08 dB.

A1.4 Fixed-frequency Horn-Gain Measurement Using Hollow-Waveguide Components.

A1.4.1 Equipment.

The equipment was the same as that used for the hollow-waveguide measurement described in Section A1.3 except that the X-axis of the recorder was driven by a voltage that was a function† of the position of the pedestal along the rails. (This voltage was obtained by a 10-turn potentiometer geared to the pedestal movement.)

A1.4.2 Procedure.

Except for the X-axis calibration, the equipment was aligned and calibrated as before. For the fixed-frequency measurement, the X-axis controls on the recorder were adjusted so that a pedestal movement of about 30 cm gave a deflection of about one major division on the X-axis. Then the separation distance was set at 150 cm.

With the generator and load directly coupled and with the oscillator tuned to successive fixed frequencies of 4.0 GHz, 4.2 GHz, etc. (as read from the dial of the oscillator), the initial signals ^{i}S were recorded by using the X-axis zero control to make a horizontal mark through a vertical division for each frequency (see Fig. 10). The initial signals are the shorter of the two horizontal marks through each vertical division. The generator and load were then connected to the antennas; 14.0 ± 0.1 dB of attenuation was removed from the rotary-vane attenuator; and the above procedure was repeated to record the final signals ^{f}S, which are the longer of the two horizontal marks through each vertical division. (While recording the initial and final signals, the system drift was checked frequently by retuning the oscillator to 4.0 GHz.)

† The X-axis deflection need be only roughly linear with the pedestal movement.

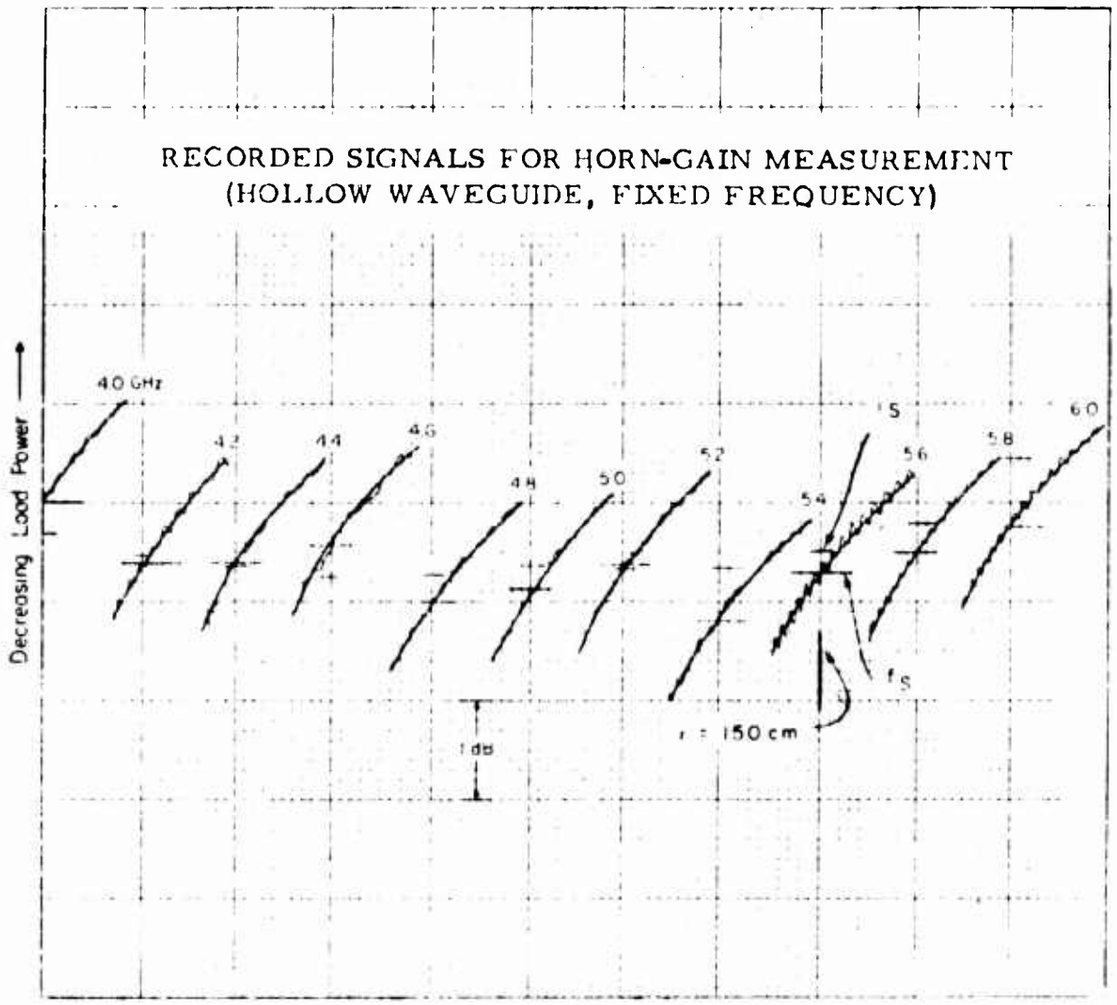

Fig. 10. Recorded Signals for Horn-Gain Measurement (Hollow Waveguide, Fixed Frequency).

Using 5.6 GHz for illustration, because the MPI was greatest for this frequency, the free-space signals ${}^fS_0$ were determined by the following procedure. The oscillator was retuned to 5.6 GHz and the X-zero control was adjusted so that the pen was directly above the vertical division corresponding to this frequency. (If any system drift had occurred, the Y-zero control was adjusted to obtain the same ${}^fS$ recorded earlier.) The pedestal was then slid away from the 150 cm position, the recorder pen was "dropped", and the pedestal was slid back through the 150 cm position to record the variation of ${}^fS$ with separation distance. The pen was lifted, and the pedestal was returned to the 150 cm position. (To eliminate any error due to "backlash" in the gearing of the potentiometer the pedestal was always moved to the 150 cm position in the same direction that it was moved to obtain the recording of ${}^fS$ versus separation distance.) The MPI perturbations on the recording of ${}^fS$ versus separation distance were averaged-out graphically as shown in Fig. 10, and ${}^fS_0$ for 5.6 GHz and r = 150 cm is given by the intersection of the resulting curve and the major vertical division. For 5.6 GHz, ${}^fS_0$ happens to be equal to ${}^fS$ at 150 cm.

From the original recording, which is on a scale of one major division per inch, it is possible to determine ${}^fS_0$ to within a few hundredths of a dB.

A1.4.3 Computing the Gain and Assigning the Uncertainty Limits.

The gain computation and the assignment of the uncertainty limits is essentially the same as in the previous examples. The results of the computation are not shown here because these gain values are less accurate than the values listed in Fig. 9. (For reasons that are unimportant here, the frequency dial of the oscillator was only accurate to within ±40 MHz for this measurement.)

A1.5 Discussion.

A1.5.1 The Periodic Gain Variations.

Referring to Figure 6 or 8, it is evident that the gain of the horns as determined from any one of the ${}^{f}S_{\theta}$ curves will have periodic variations of about 0.4 dB, peak-to-peak, as a function of frequency. Even though these variations are not much outside the stated uncertainty limits for these gain measurements, it is known from some further experimentation that the indicated gain variations are real. (Six independent gain measurements performed on these same horns have each shown almost identical variations despite radical differences in the matching conditions at the generator and load ports and in the range configuration.) The theoretical gain values for these horns (expressed in dB) are almost linear with frequency, and the measured gain values display roughly sinusoidal variations around the theoretical values.

In one series of experiments, various amounts of slightly-lossy foam were placed inside each horn between the aperture and throat. These absorbing "plugs" reduced the large, long period variations in ${}^{f}S_{\theta}$ considerably, which suggests strongly that the variations are caused by an interaction between the aperture and throat of each horn. Although this interaction would actually be quite complicated, the period of the gain variations is consistent with the interpretation of this interaction as being qualitatively the same as the interaction between two waveguide discontinuities separated by the aperture-to-throat distance. By the same procedure used to derive (27), the period of this variation should then be given approximately by

$$\Delta f_{v} \approx \frac{3}{20L} \qquad (38)$$

where Δf_{v} is the frequency change in GHz corresponding to one period and L is the length of the flared portion of the horn in meters. For the horns used in these measurements L is about 0.25 meters, and (38) would predict a period of 0.6 GHz for the gain (or insertion-loss) variations. This prediction is in surprisingly good agreement with Figures 6 and 8, and (38)

also provides equally accurate predictions of the period of the gain variations for the other "NRL"[12] design horns.

A1.5.2 Measurement Design.

The measurements discussed here were based on the design formulas presented in Section 4. Some recapitulation of the design criteria for the swept-frequency gain measurements may be of interest.

The gain variations discussed in the last paragraph are particularly troublesome. Because of them, it is a practical necessity to use swept-frequency techniques to accurately determine the gain of small horns over their full bands; but the gain variations also make the swept-frequency gain measurements more difficult. The MPI perturbations should have much shorter periods than the gain variations if the MPI perturbations are to be easily recognizable and thus averaged out without ambiguity. This means that the path-length differences for all of the significant MPI components must be several times larger than twice the flare-length of the horns (twice the longer flare-length if the horns are different). In other words, the frequency change Δf required to produce a perturbation cycle for any MPI component must be several times smaller than Δf_v given by (38).

Considering the mutual MPI for the horns under discussion here, which have flare-lengths of about 0.25 meters, (27) shows that Δf_s will be about one fourth of Δf_v at a separation of only 100 cm.† However, (22)

† Referring to the 'S curve for 100 cm in Fig. 6, it will be noted that Δf_s is actually about 0.1 GHz rather than 0.15 as predicted by (27). If the throat-to-throat distance rather than the aperture-to-aperture distance is used for s in (27), then the predicted and observed values for Δf_s agree closely. This appears to be true for pyramidal horns in general and suggests that the scattering occurs, predominantly, near the throats of these horns.

indicates that the magnitude of the mutual MPI perturbations at 100 cm, which is about a^2/λ for 6 GHz, could be as large as ± 0.5 dB; so a larger separation distance is desirable. Considering the MPI from the floor or ceiling, each about 1.5 meters from the transmission axis, (26) shows that Δf_1 will be less than one fourth of Δf_4 if the separation distance is less than 1.5 meters. From the patterns of these horns[12] and from (18), the interference level for either the floor or ceiling component should be no larger than -45 dB, which corresponds ± 0.05 dB perturbations, for separation distances out to 200 cm. As brought out in the next two paragraphs, the other sources of MPI should be less troublesome than the three components discussed so far. It follows then that a separation distance of about 150 cm, and probably out to about 200 cm also, should produce the best results for this measurement. These predictions are confirmed fairly well by Fig. (6).

The path-length differences for all of the MPI components from the side directions were at least as great as the path-length differences for the ceiling and floor components, which insures that the perturbation period for these components is short enough. The MPI level for the scattering components from the side directions should be quite small for the following reasons: the walls of the room were far enough away to be relatively unimportant as sources of interference; to a large extent the walls of the room were hidden behind benches, cabinets, etc., which tended to produce a number of very small interference components from the side directions rather than two larger components; and the horns were oriented with vertical polarization so that the transmission and reception in the side directions was greatly reduced due to the H-plane pattern levels, which are much lower than the E-plane pattern levels for these horns for angles greater than 30 degrees.

Consider the field that is scattered back to the transmitter region from the absorbing wall behind the receiving aperture and then rescattered to the receiver from the transmitting antenna and the absorbing

wall behind the transmitting aperture. Unless the absorbing walls are moved with respect to the antennas, this MPI component will be essentially indistinguishable from the mutual MPI component because it will have essentially the same perturbation period as the mutual MPI component. This MPI component (which is due to multiple, back-and-forth scattering) is usually not significant when high performance absorbing materials are used for the walls, and it would not be a problem even if it were not negligible because its perturbation period is sufficiently small. However, fields scattered directly from the absorbing walls to the receiving aperture can be a problem if the back-lobes of the patterns of the antennas are not small. Consider (1) the back-lobe radiation from the transmitting aperture that is scattered directly to the receiving aperture from the absorbing wall behind the transmitting aperture and (2) the directly scattered radiation from the absorbing wall behind the receiving aperture that is received due to the back-lobe of the receiving aperture. These MPI components can be very troublesome because their perturbation periods will be long (approximately the same as the period of the gain variations). Even though the level of such interference should be insignificant for most horn gain measurements, and this one in particular, it should be definitely established by experiment that such interference is insignificant. This is easily done, provided that the absorbing walls have been constructed so that they are movable, by moving the absorbing walls with respect to the horns to introduce phase reversals for these MPI components. This was done for the gain measurements described here, and no interference perturbations could be detected.

A1.5.3 Improvements.

There are several obvious improvements that can be made in the range, equipment, and procedure to obtain higher accuracy gain measurements:

(1) The use of a larger range will not only reduce the uncertainty associated with the near-zone correction but will reduce the uncertainty involved in averaging out the MPI perturbations in ^{f}S because the period of these perturbations will then be smaller.

(2) The need for the calibrated RF attenuator can be avoided by using a detecting and metering system with sufficient dynamic range (about 20 dB). The dynamic range of the system used here was only about 10 dB (for a 0.01 dB deviation from square-law response of the crystal), and there are a number of simple detecting and metering systems that will provide at least a 10 dB improvement over this system. In addition to avoiding the fairly large uncertainty associated with the RF attenuator, the use of a suitable insertion-loss measuring system can also achieve a smoother ^{i}S curve, which is quite important for the following reasons. Most of the "lumps" in the ^{i}S curves in Fig. 6 and Fig. 8 are caused by the attenuator-isolator combination. These same "lumps" should also show up in the $^{f}S_{o}$ curves; however, because the length of these lumps is comparable to the period of the MPI variations, these lumps cannot be accurately resolved for some frequencies. For instance, referring to Fig. 6, the lump at 4.24 GHz is not accurately resolved on the $^{f}S_{o}$ curves. By contrast, the lump at 4.46 GHz is fairly well resolved because the MPI perturbations are small for this frequency.

(3) Electronically tunable band-pass filters using yttrium-iron-garnets ("YIG" filters) are commercially available that can be made to track the fundamental frequency of the sweep oscillator over octave

frequency sweeps. Thus, uncertainties due to spurious frequencies and harmonic frequencies can be effectively eliminated.

(4) Automatic electronic frequency meters are commercially available that can be used to drive the X-axis of the recorder to provide a very accurate, direct reading, frequency axis.

(5) The uncertainties that arise because of a "lumpy" ${}^{i}S$ curve, discussed under (2) above, can be avoided by subtracting ${}^{i}S$ from ${}^{f}S$ before averaging out the MPI perturbations. That is the MPI perturbations would be averaged out from the quantity 10 log $({}^{f}P_{L}/{}^{i}P_{L})$ as given by equation (33). If an analog to digital converter is used to digitize the initial and final load power signals, this procedure can be done by computer and the MPI perturbation averaging and gain calculation can also be done by computer.

A2. Determining $P_{L\theta}$ by Averaging the Perturbations in the Received Power.

The discussion in this appendix concerns the inherent inaccuracies involved in determining $P_{L\theta}$ by simply averaging out the MPI perturbations in the received power. That is, a perfectly regular perturbation is assumed, and only the accuracy of the averaging process is considered.

Provided that the perturbations in the received power are no larger than about $\pm$ 0,5 dB, there is little error involved in obtaining $P_{L\theta}$ by averaging the extrema of the perturbations. Furthermore, either the load power or the load power expressed in dB can be averaged to obtain $P_{L\theta}$. The qualitative truth of these statements is evident, but a numerical example should be worked out to establish the limits of accuracy involved.

For simplicity, assume that only one interference voltage is present. Using 10 Log $P_{L\theta}$ as a reference, the curve in Fig. 11 illustrates the approximately sinusoidal variation in 10 Log P_L around 10 Log $P_{L\theta}$ as the phase angle θ is varied by 360 degrees. Specifically, the curve of Fig. 11 is for an interference voltage level $K = 0.06$, which corresponds to a power interference ratio (PIR) $= p = 1.0436$ dB. The upper dashed line in Fig. 11 represents 10 Log $P_{L\theta}$ as determined by averaging the extrema of the load power and expressing this average in dB. The lower dashed line represents 10 Log $P_{L\theta}$ as determined by averaging the extrema of 10 Log P_L. (The "perfect" symmetry of the dashed lines with respect to 10 Log $P_{L\theta}$ is not "real", it is due to round-off.)

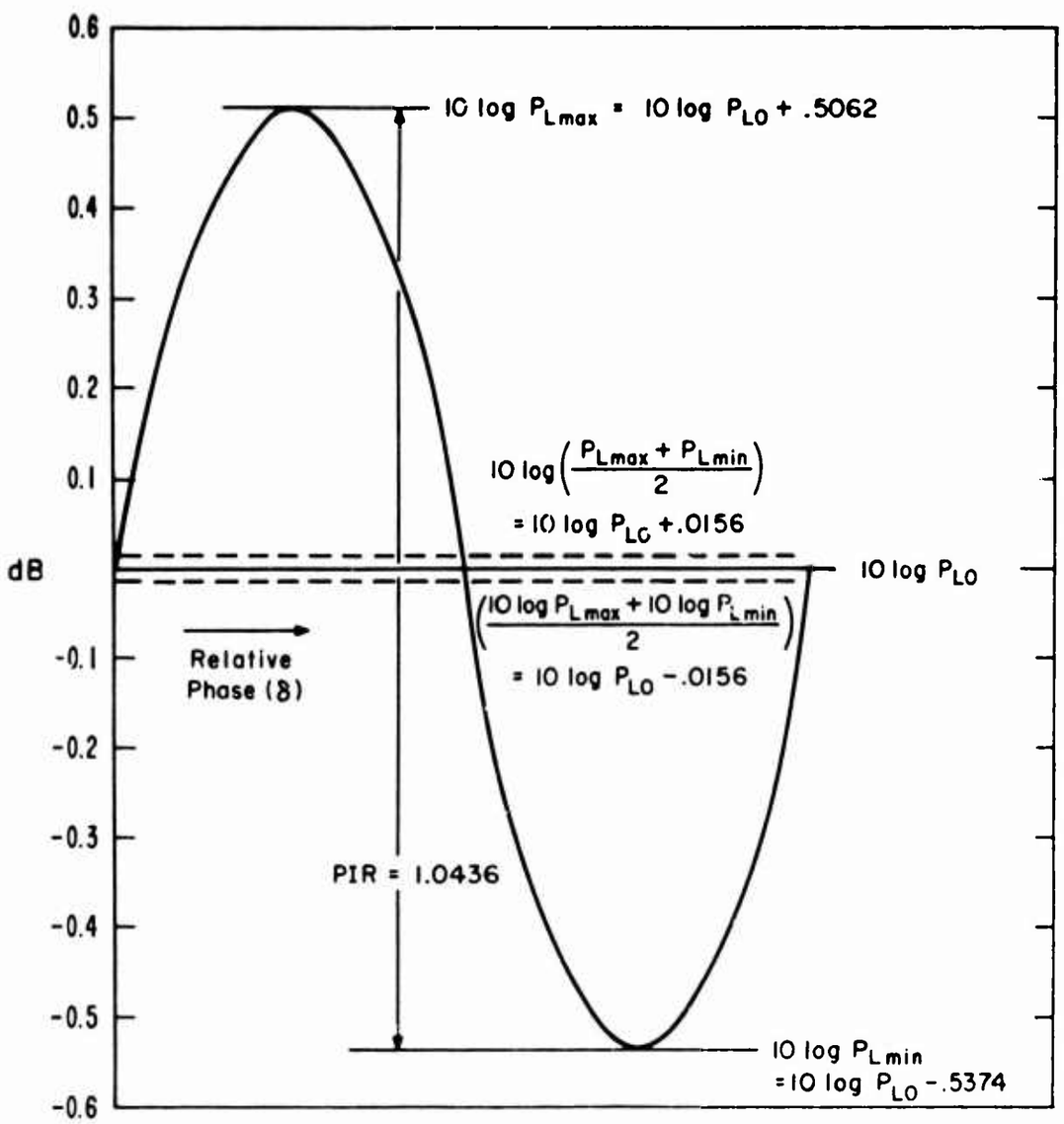

Figure 11. Illustration of the Inaccuracies Involved in Determining P_{LO} by Averaging the Extrema of the MPI Perturbations in the Received Power.

A3. Boresight Errors Due to Multipath Interference.

During the gain measurements discussed in Section A1, the receive horn was rotated through plus and minus five degrees in both the E-plane and H-plane to determine the power variation as a function of the direction angles. For these measurements the separation distance was 150 cm, and the back-and-forth scattering between the antennas is by far the largest source of multipath interference for this separation. For simplicity of discussion it will be assumed that the mutual MPI is the only interference component.

Due to the construction of the antenna rotator and the antenna mounting brackets, neither axis of rotation passed through the phase center of the antenna. Therefore, significant changes in the separation distance occurred as a result of the antenna rotation. The axis for the H-plane rotation passed through the antenna transmission axis (about 40 cm behind the aperture), which means that the change of separation distance with H-plane rotation will be zero in the boresight direction. Therefore, there should be no phase changes between the direct component and the mutual MPI component that would affect the "boresighting" in the H-plane. This proved to be true, and the H-plane boresight direction agreed to within about 0.1 degree with the geometric axis of the antenna. However, the axis for the E-plane rotation passed through a point about 40 cm behind the aperture plane and about 25 cm below the transmission axis. This means that the mutual MPI component will undergo about a 180 degree phase change for a five degree rotation in the E-plane. The corresponding effect on the E-plane boresight direction is shown in Fig. 12 for four frequencies. Two of these frequencies, 4.8 GHz and 5.0 GHz, were chosen because the mutual MPI component is small for these frequencies; and, as expected, the boresight direction agrees closely with the geometric axis. The 5.6 GHz and 5.8 GHz frequencies were chosen because the mutual MPI component is large for these

frequencies, and Fig. 12 shows that the boresight direction differed by about 1 degree from the geometric axis for 5.6 GHz.

Figure 13 shows the MPI perturbations in the received power for frequency sweeps for a number of E-plane rotation angles. (Merely to separate the curves for better display, the Y-axis zero was adjusted by about 1 dB for each degree of rotation.) In particular, the changes in the MPI perturbation with rotation angle at 5.6 GHz should be noted.

When making gain measurements in the near-zone, it is good practice to align horn antennas geometrically. If it is necessary to align them by "peaking" the received power, it is important that the rotation axes pass through the transmission axis (at a point as near as practicable to the phase center of the antenna and that the boresighting be accomplished using a frequency for which the MPI level is minimum.

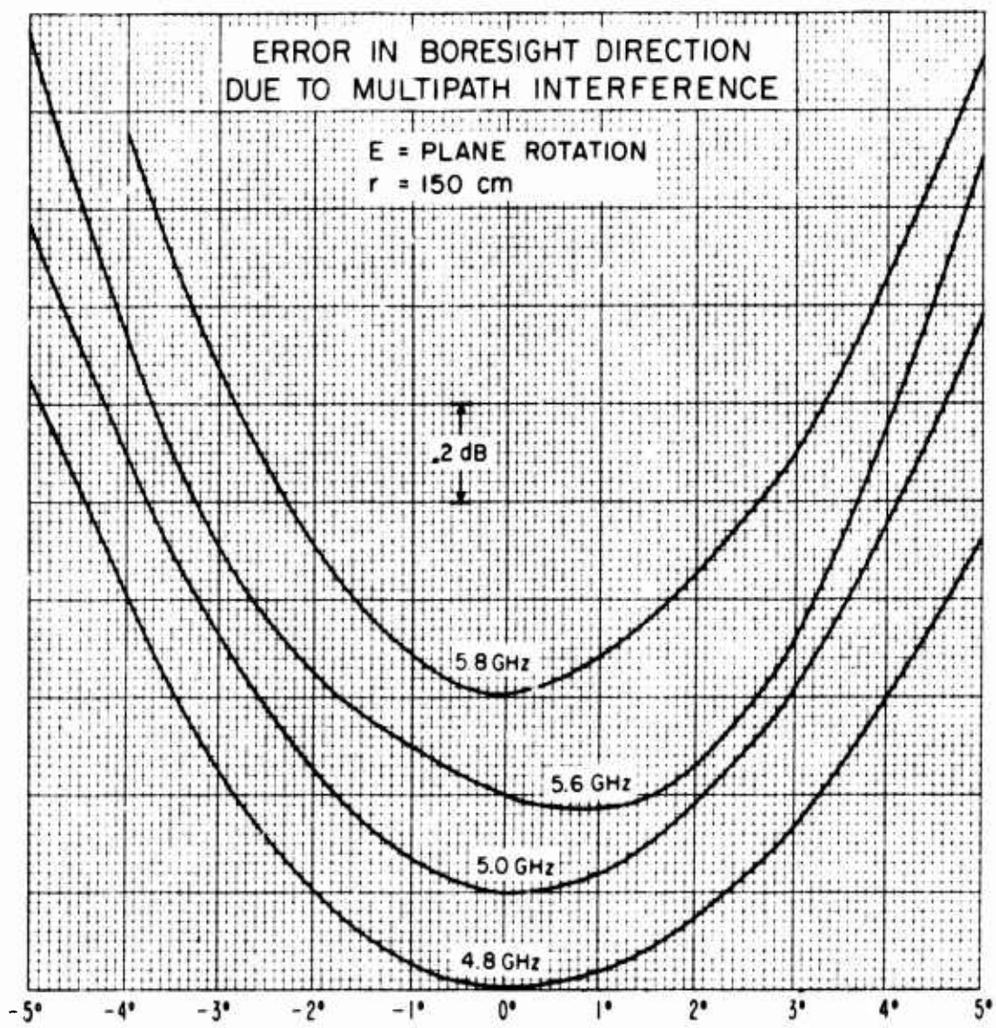

Fig. 12. Error in Boresight Direction Due to Multipath Interference.

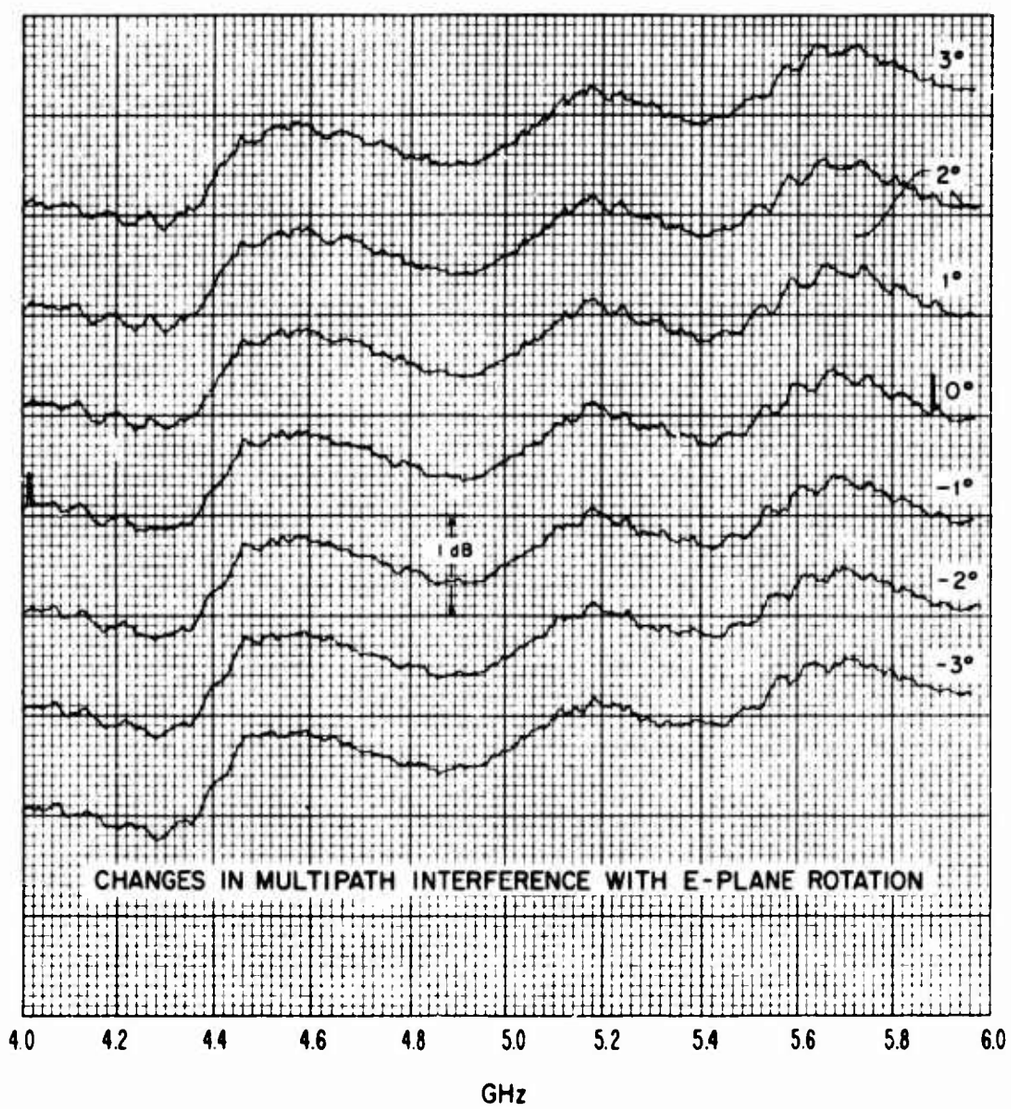

Fig. 13. Changes in Multipath Interference with E-Plane Rotation.

A4. Near-Zone Correction Data.

Figures 15 and 16 were obtained by graphing the tabular data provided by Chu and Semplak. (If the reader refers to Chu and Semplak's paper, it should be noted that symbols used for the parameters in Figures 15 and 16 are different from those used by Chu and Semplak.)

Figures 15 and 16 are applicable only to the case of power transfer between identical pyramidal horns. The gain correction (5 log N) for each horn is the sum of the H-plane and E-plane corrections. Referring to Fig. 14, the E and H parameters are computed from the aperture dimensions and the slant heights. The horizontal axis in Figures 15 and 16 are the logarithims of the separation distance expressed in Rayleigh lengths corresponding to the aperture dimensions a and b respectively.

For swept-frequency gain measurements, one wishes to know the gain correction as a function of frequency at some fixed distance suitable for the measurement. Figures 17 through 22 show the gain corrections as a function of frequency for the commonly used "NRL" design horns. These graphs were obtained by using Figures 15 and 16. The separation distances used for each graph correspond, roughly, to a^2/λ, $1.5a^2/\lambda$, and $2a^2/\lambda$ for the upper end of each frequency band.

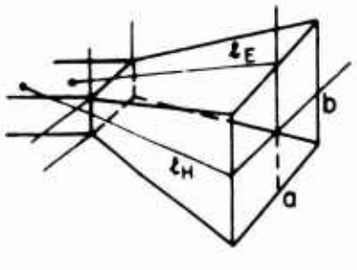

Fig. 14. Antenna Dimensions.

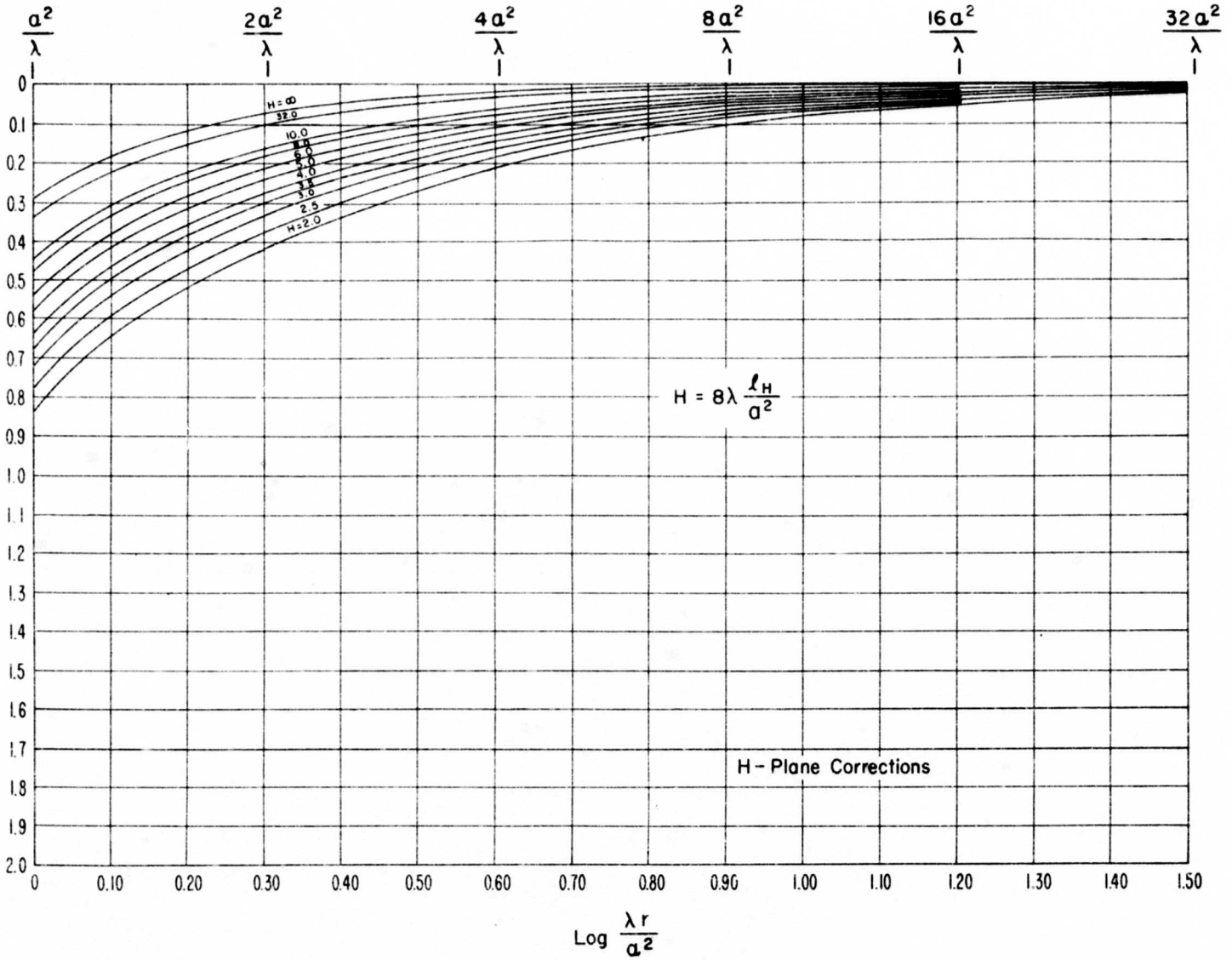

Fig. 15. H-Plane Gain Corrections.

B-73372

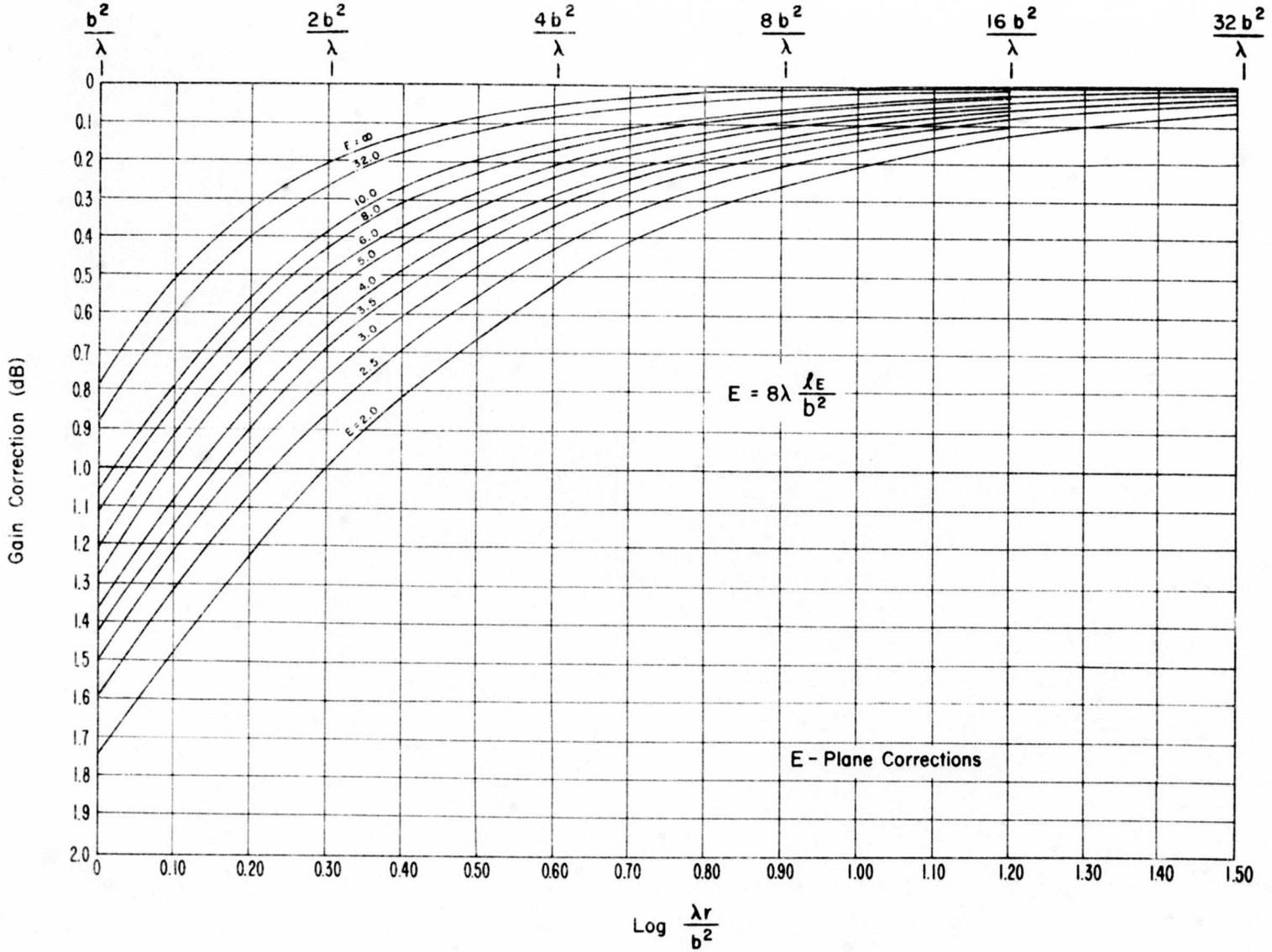

Fig. 16. E-Plane Gain Corrections.

73371

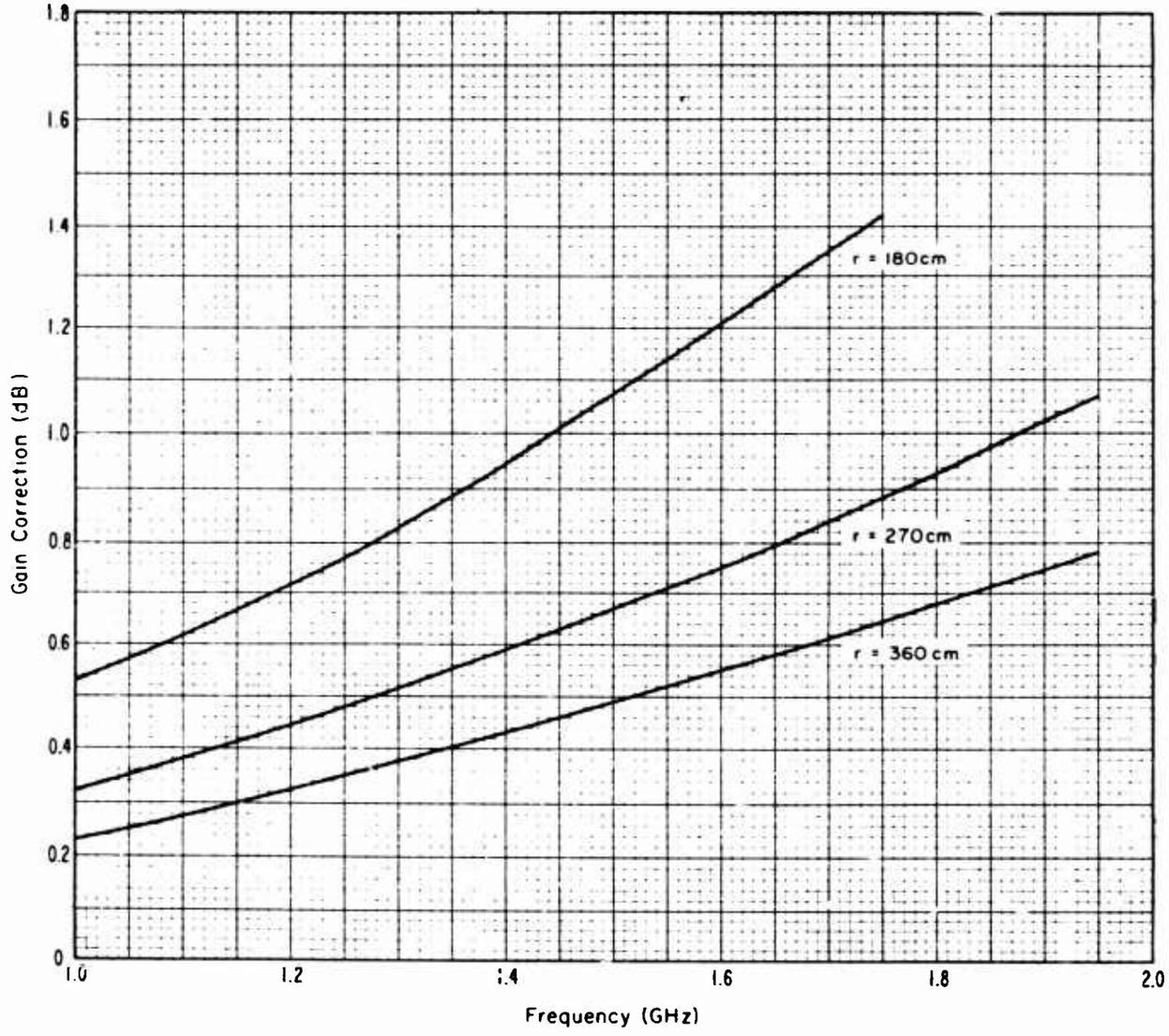

Fig. 17. Gain Corrections for "NRL" Design 23 cm Band Horn (1.12 GHz to 1.70 GHz).

73225

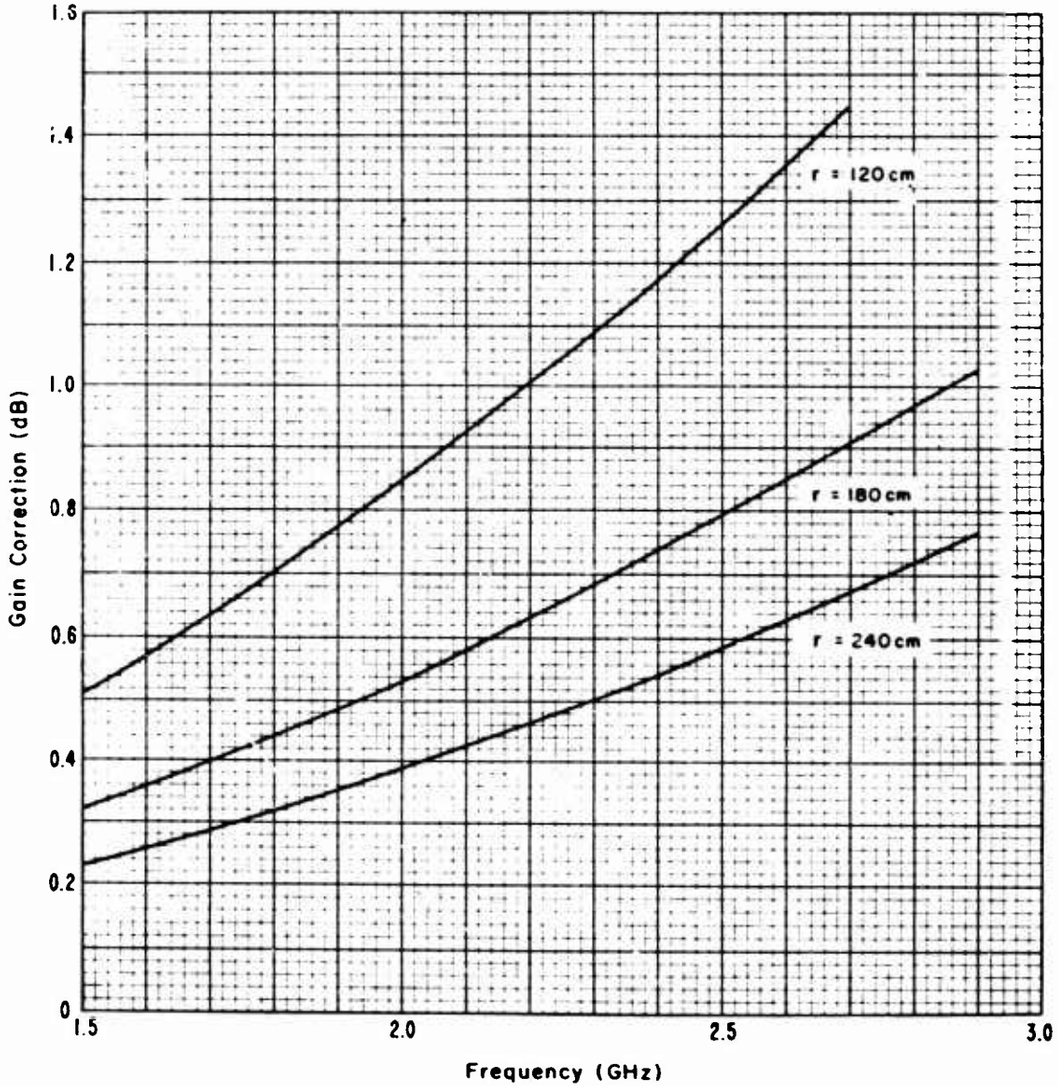

Fig. 18. Gain Corrections for "NRL" Design 15 cm Band Horns (1.70 GHz to 2.60 GHz).

73226

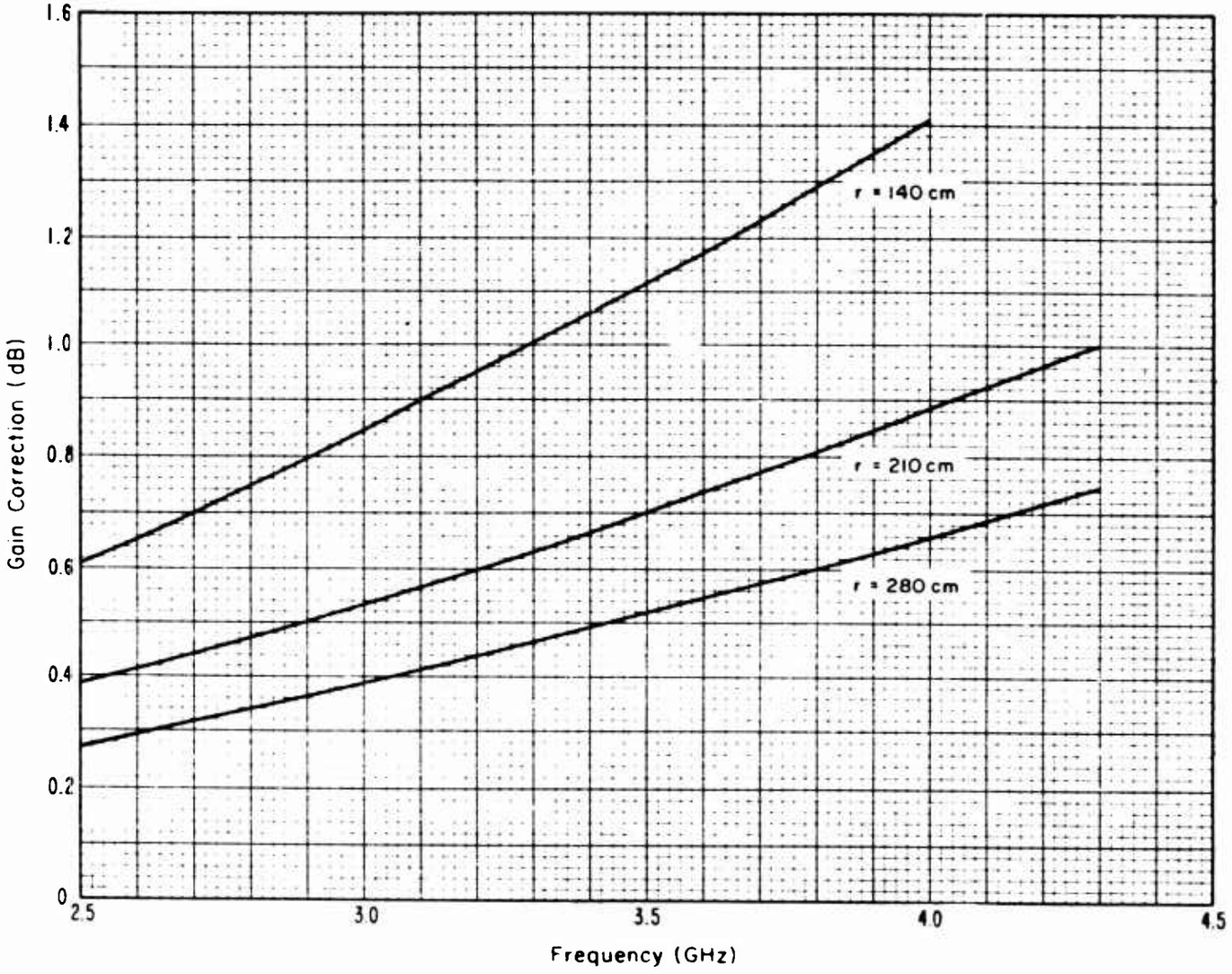

Fig. 19. Gain Corrections for "NRL" Design 10 cm Band Horns (2.60 GHz to 3.95 GHz).

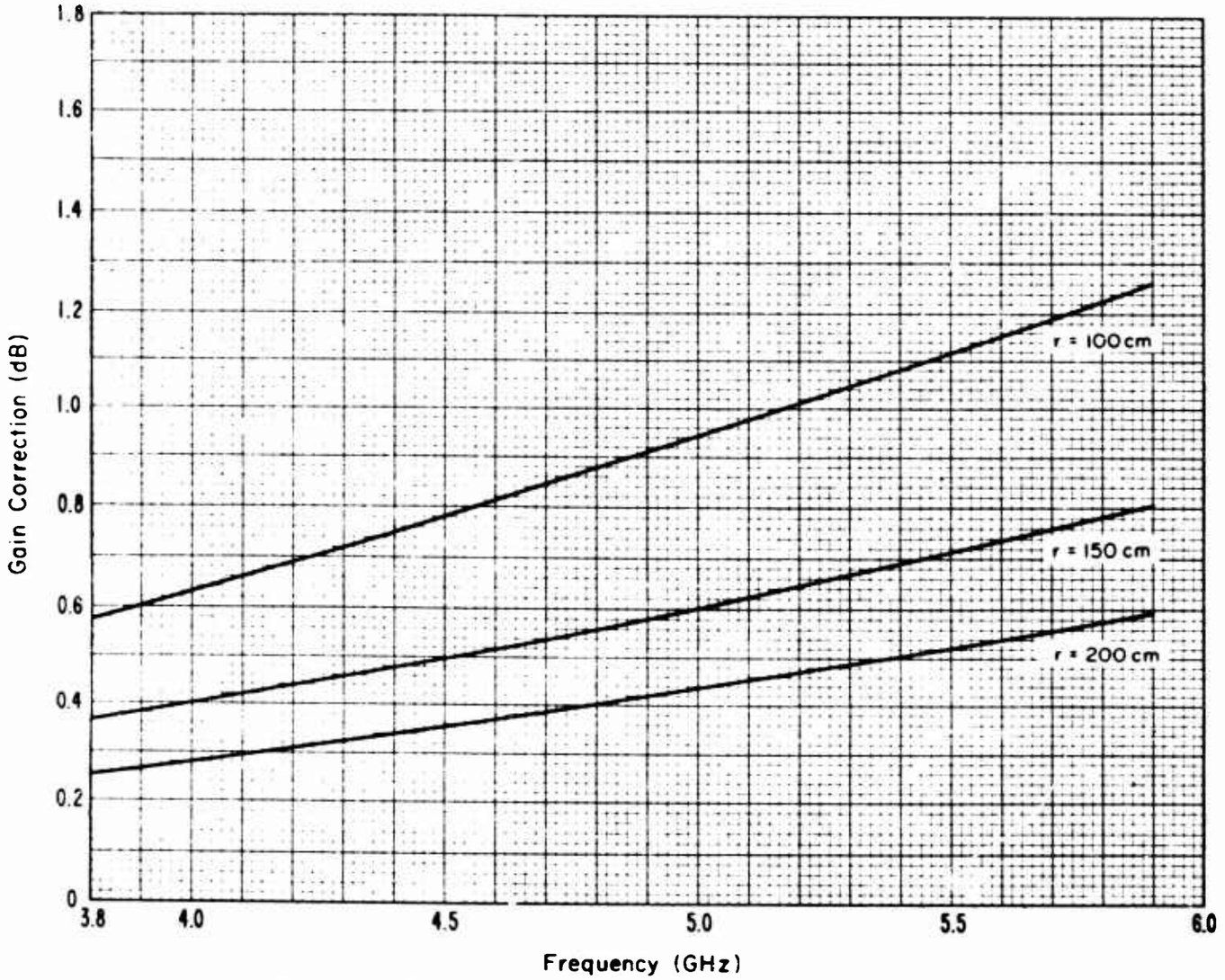

Fig. 20. Gain Corrections for "NRL" Design 6 cm Band Horns (3.95 GHz to 5.85 GHz).

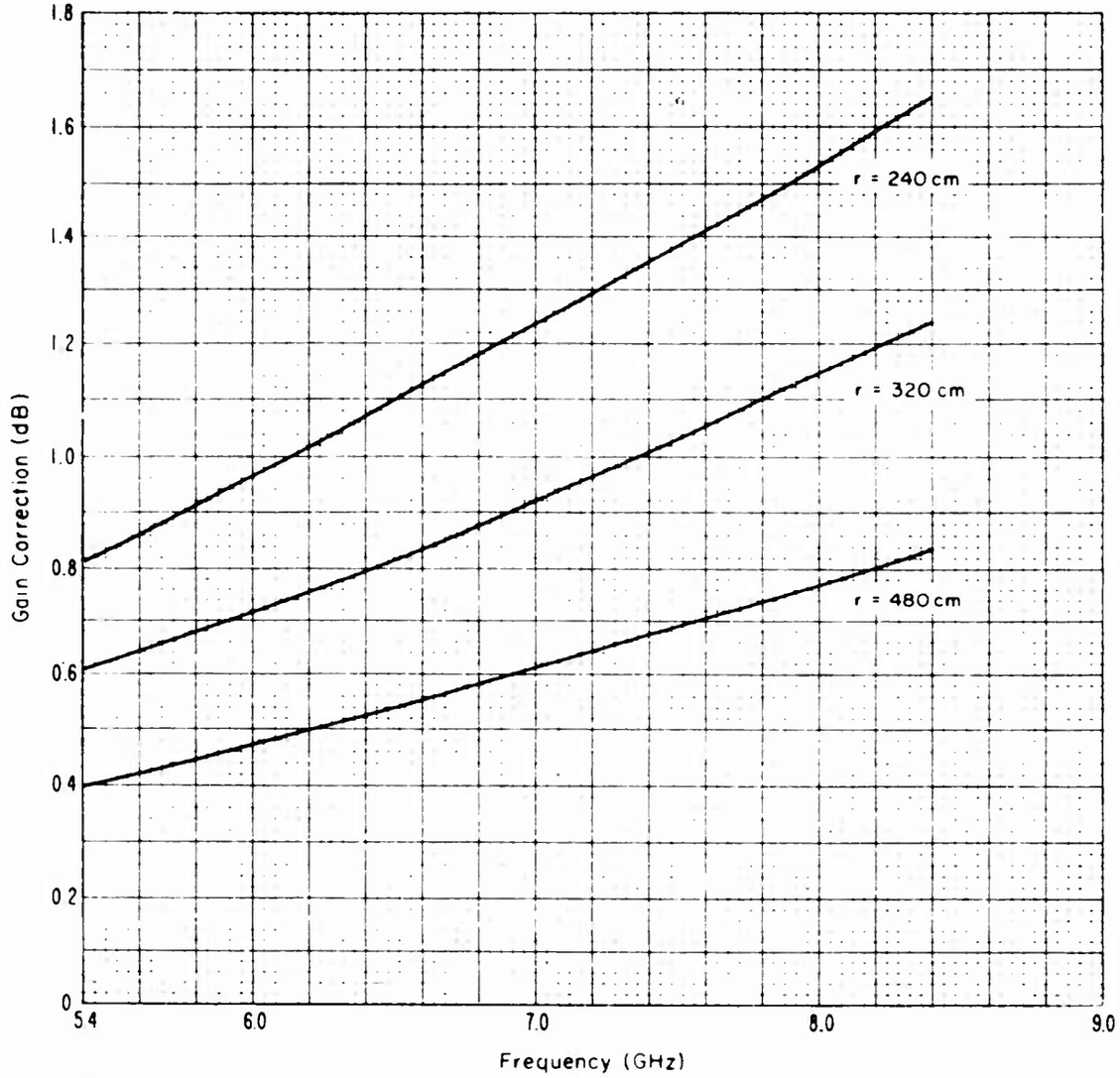

Fig. 21. Gain Corrections for "NRL" Design 4.75 cm Band Horns (5.85 GHz to 8.20 GHz).

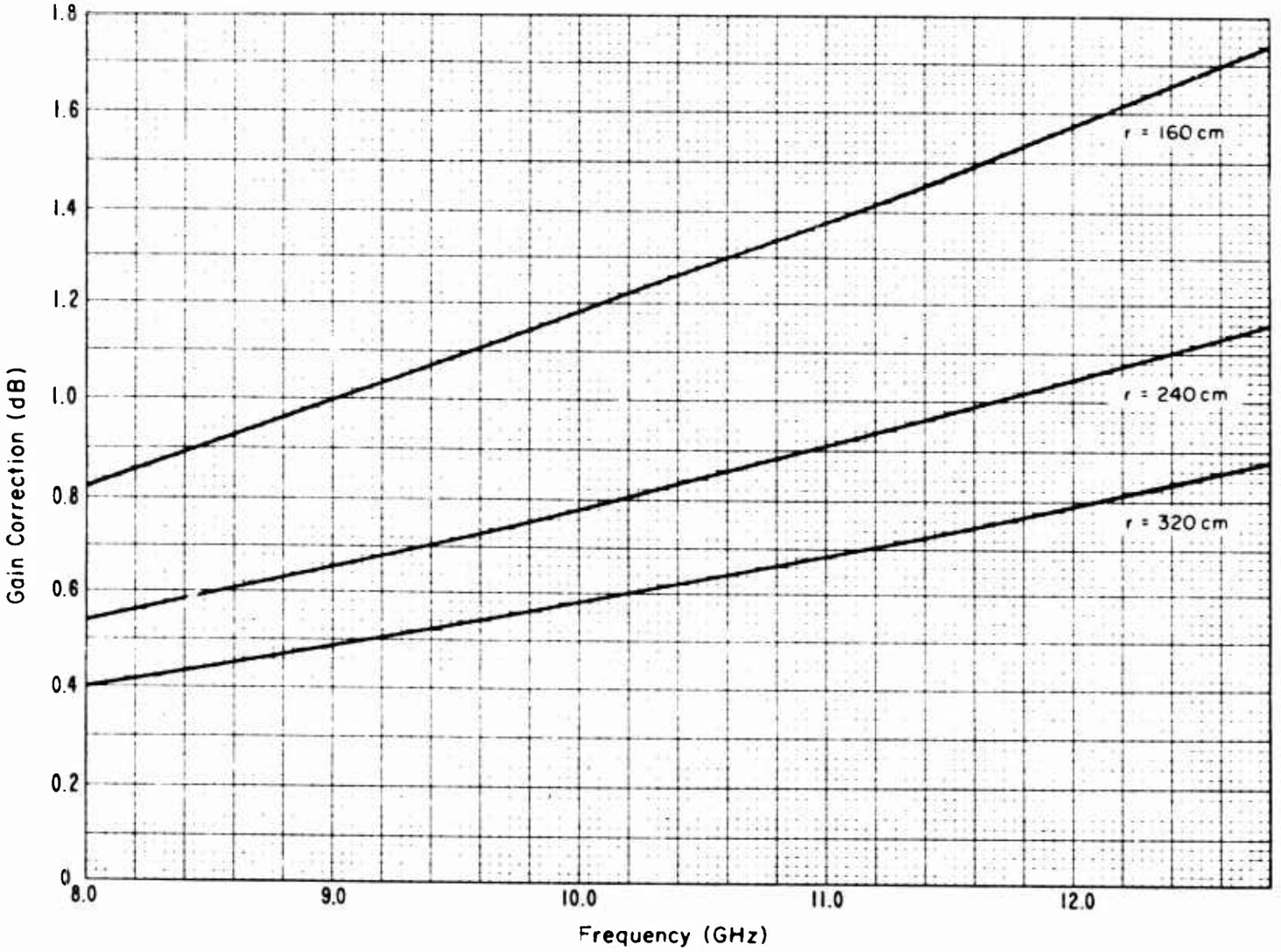

Fig. 22. Gain Corrections for "NRL" Design 3.2 cm Band Horns (8.20 GHz to 12.40 GHz).

REFERENCES

[1] Beatty, R.W. (June 1964), Insertion loss concepts, Proc. IEEE 52, 663-671.

[2] Kerns, D.M. and R.W. Beatty (1967), Basic Theory of Waveguide Junctions and Introductory Microwave Network Analysis (Pergamon, New York).

[3] Bowman, R.R. (June 1967), Field strength above 1 GHz: Measurement procedures for standard antennas, Proc. IEEE 55, 981-990.

[4] Beatty, R.W. (March 1967), Discussion of errors in gain measurements of standard electromagnetic horns, NBS Tech. Note 351.

[5] Tai, C.T. (March 1961), On the definition of the effective aperture of antennas, IRE Trans. on Antennas and Propagation (Communications) AP-9, 224-225.

[6] IEEE Test Procedure for Antennas, No. 149 (Revision of 48 IRE 2S2)(Jan. 1965), IEEE Trans. on Antennas and Propagation, AP-13, 437-466 (May 1965).

[7] Ely, P.C., Jr. (June 1967), Swept-frequency techniques, Proc. IEEE, 55, 991-1002.

[8] Engen, G. F. (April 1958), Amplitude stabilization of a microwave signal source, IRE Trans. on Microwave Theory and Techniques, MTT-6, 202-206.

[9] Braun, E.H. (Jan. 1953), Gain of electromagnetic horns, Proc IRE, 41, 109-115.

[10] Chu, T.S. and R.A. Semplak (March 1965), Gain of electromagnetic horns, Bell Sys. Tech. J., 527-537.

[11] Tseytlin, V.B. and B.Y. Kinber (Jan. 1965), Measurement of the directive gain of horn antennas at a short distance, Radio Engrg. and Electronic Phys. 10, 10-16.

[12] Slayton, W.T. (Nov. 1954), Design and calibration of microwave antenna gain standards, Naval Research Lab., Washington, D.C. Rept. 4433.

[13] Hu, M.K. (1958), Near-zone power transmission formulas, IRE Nat'l. Conv. Rec., pt. 8, 128-135.

[14] Jull, E.V. and R.R. Bowman (Feb. 1968), Electromagnetic horn gain measurements, Proc. IEEE, 56, 215-216.

[15] Fitzgerrell, R.G. (March 1966), Swept-frequency antenna gain measurements, IEEE Trans. on Antennas and Propagation, AP-14, 173-178.

[16] Moeller, A.W. (March 1966), The effect of ground reflections on antenna test range measurements, Microwave Journal, 9, no. 3, 47-54.

[17] Jull, E.V. and Deloli, E.P., An accurate absolute gain calibration of an antenna for radio astronomy, IEEE Trans. on Antennas and Propagation, vol. AP-12, pp. 439-447, July, 1964.

[18] Eisenhart, C., Realistic evaluation of the precision and accuracy of instrument calibration systems, J. Research NBS, vol. 67C, April-June 1963.

[19] Powers, R.S., Maximum use of existing accuracy in measurements, NBS Report 9706, April 1, 1968.

UNCLASSIFIED

Security Classification

DOCUMENT CONTROL DATA - R & D

(Security classification of title, body of abstract and indexing annotation must be entered when the overall report is classified)

1. ORIGINATING ACTIVITY (Corporate author)	2a. REPORT SECURITY CLASSIFICATION
National Bureau of Standards Radio Standards Engineering Division Boulder, Colorado 80302	Unclassified 2b. GROUP

3. REPORT TITLE

ABSOLUTE GAIN MEASUREMENTS FOR HORN ANTENNAS

4. DESCRIPTIVE NOTES (Type of report and inclusive dates)

Final Report Jan 1967 - Jul 1968

5. AUTHOR(S) (First name, middle initial, last name)

Ronald R. Bowman

6. REPORT DATE	7a. TOTAL NO. OF PAGES	7b. NO. OF REFS
November 1968	88	19

8a. CONTRACT OR GRANT NO.	9a. ORIGINATOR'S REPORT NUMBER(S)
F30602-67-C-0163 b. PROJECT NO. 4540 Task No. 454001 d.	9b. OTHER REPORT NO(S) (Any other numbers that may be assigned this report) RADC-TR-68-349

10. DISTRIBUTION STATEMENT

This document is subject to special export controls and each transmittal to foreign governments, foreign nationals or representatives thereto may be made only with prior approval of RADC (EMCVM-1), GAFB, N.Y. 13440.

11. SUPPLEMENTARY NOTES	12. SPONSORING MILITARY ACTIVITY
	Rome Air Development Center (EMCVM-1) Griffiss Air Force Base, New York 13440

13. ABSTRACT

A detailed discussion is presented of absolute gain measurements by the insertion-loss method (also known as the "two-antenna" or "three-antenna" method). The discussion emphasizes error analysis, electrical mismatch, near-zone corrections, swept-frequency gain measurements, and techniques for experimentally reducing the effects of multipath interference. Some simple terms, concepts, and formulas are presented that are useful for the design and evaluation of antenna or field strength measurements when multipath interference is involved. It is concluded that swept-frequency horn-gain measurement with uncertainty limits of less than ± .1 dB can be made on small indoor ranges. Examples of horn-gain measurements are included.

plus or minus

DD FORM 1 NOV 68 1473

UNCLASSIFIED

Security Classification

14 KEY WORDS	LINK A		LINK B		LINK C	
	ROLE	WT	ROLE	WT	ROLE	WT
Antennas Antenna Feeds Horn Antennas Antenna Gain						